Production of nuclei via correlated decay of nuclear sources in local equilibrium

Alexander Botvina

ITP, Goethe University, Frankfurt am Main , Germany

(collaboration with M.Bleicher, N.Buyukcizmeci, R.Ogul, W.Trautmann)

NUSYM23 - XIth International Symposium on Nuclear Symmetry Energy, 18-22 September, 2023, GSI, Darmstadt, Germany

Qualitative picture of dynamical stage of the reaction leading to fragment production (e.g., UrQMD calculations)

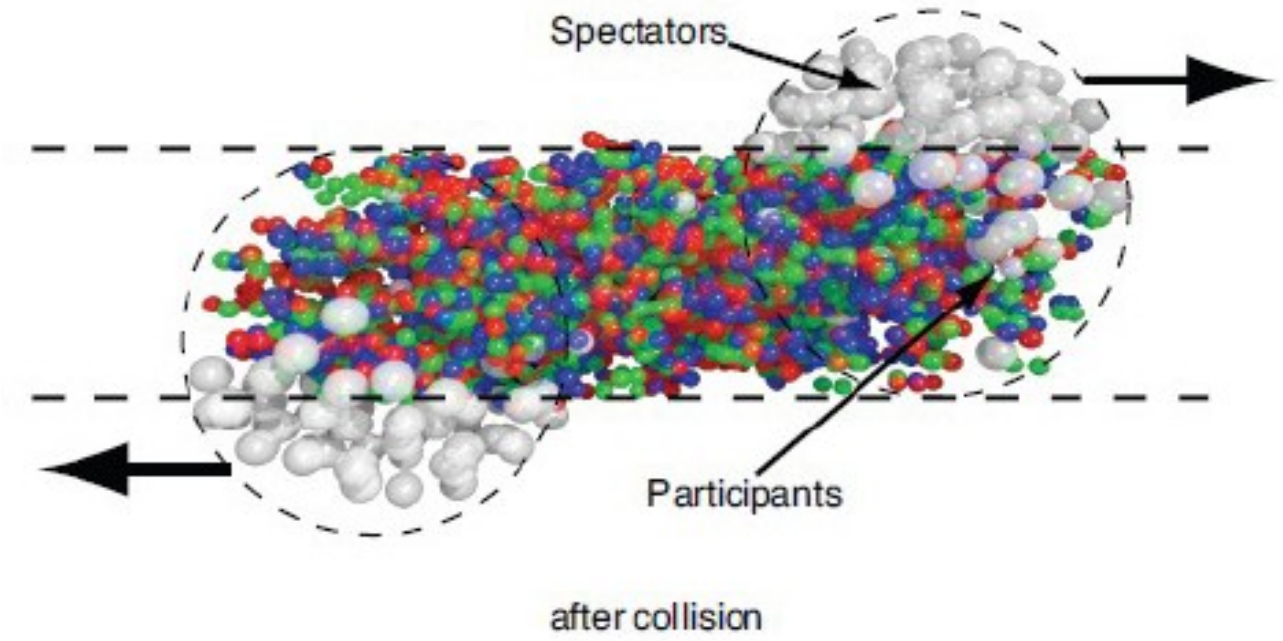

Fragment formation is possible from both participant nucleons and spectator residues

The formation of nuclear fragments in collisions of nuclei is a many-body process, there is no a dominating channel. The theoretical explanation requires both dynamical and statistical approaches.

It can be subdivided into two main stages:

1) Dynamical stage leading the production of new baryons at the diluted density (+ in some cases, lightest nuclei) and excited equilibrated nuclear systems, e.g., nuclear residues.

2) Statistical disassembly of the systems consisting of many baryons (including the nuclear residues) , which leads to the production of final nuclei.

Formation of baryon clusters from the dynamically produced baryons as a results of secondary interaction between them, when they are in the vicinity of each other. Note: baryons in clusters can come to equilibrium and the clusters are excited respective to its ground state. This case is realized in Heavy- Ion collisions of medium/high energies.

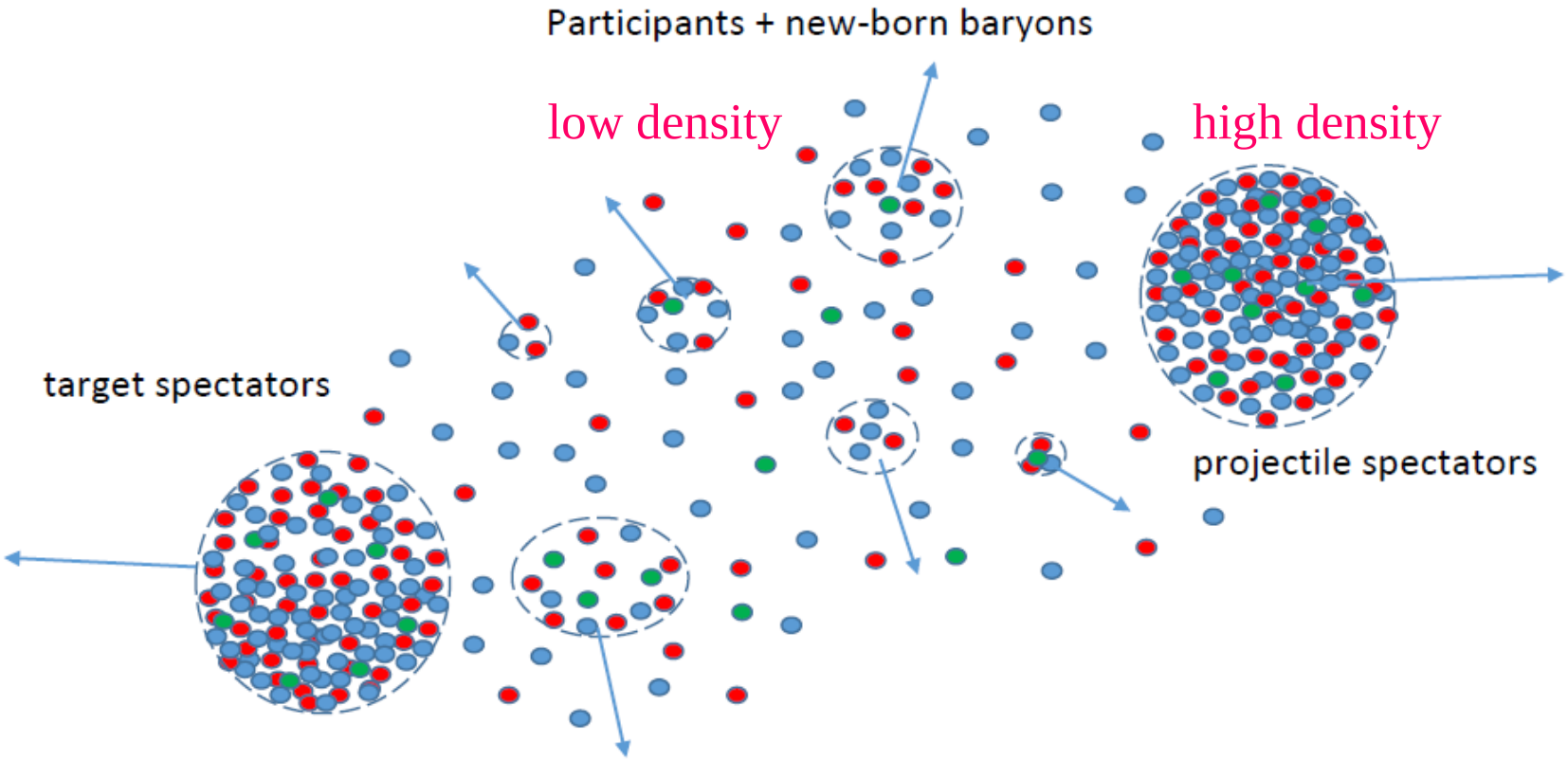

Formation of baryon clusters from the dynamically produced baryons as a results of secondary interaction between them, when they are in the vicinity of each other. Note: baryons in clusters can come to equilibrium and the clusters are excited respective to its ground state. This case is realized in Heavy- Ion collisions of medium/high energies.

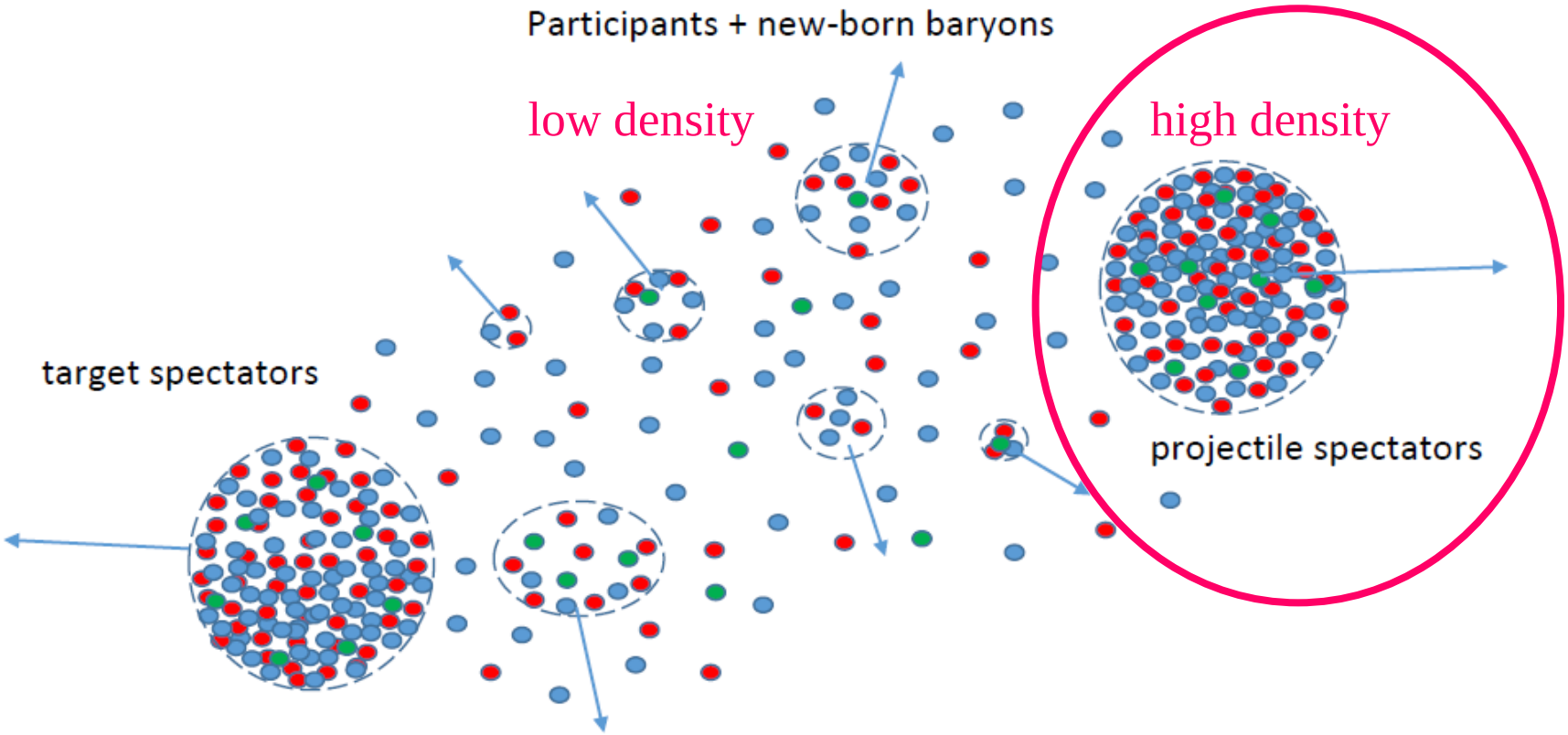

Low/intermediate energies: hadron/lepton collisions with nuclei, + mechanisms for peripheral ion collisions – spectator residues

Dinamical stage with particle emission and production of excited nuclear residues

Preequlibrium emission + equilibration

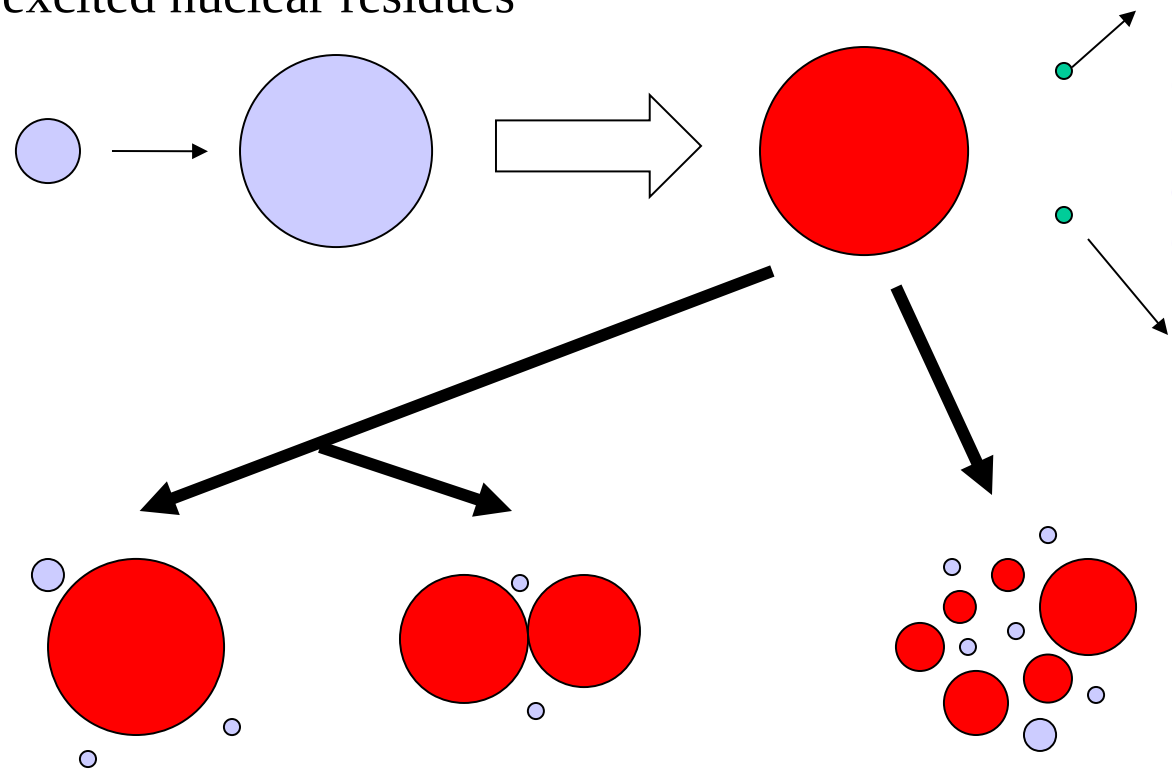

evaporation fission multifragmentation

Statistical approach

N.Bohr (1936)

Compound-nucleus decay channels (sequential evaporation or fission) dominate at low excitation energy of thermal sources E^*<2-3 MeV/nucl

N.Bohr, J.Wheeler (1939)
V.Weisskopf (1937)

starting 1980-th, conception: statistical freeze-out volume

At high excitation energy E^*>3-4 MeV/nucl there is a simultaneous break-up into many fragments (e.g. SMM: Phys.Rep.**257**(1995)133)

Production of large nuclear fragments in reactions after fusion (central collisions) of colliding nuclei at low- and intermediate-(Fermi)energies:

Formation of a single excited source after pre-equilibrium emission of light particles.

These reactions were related to the idea of investigating nuclear phase transition in multifragmentation

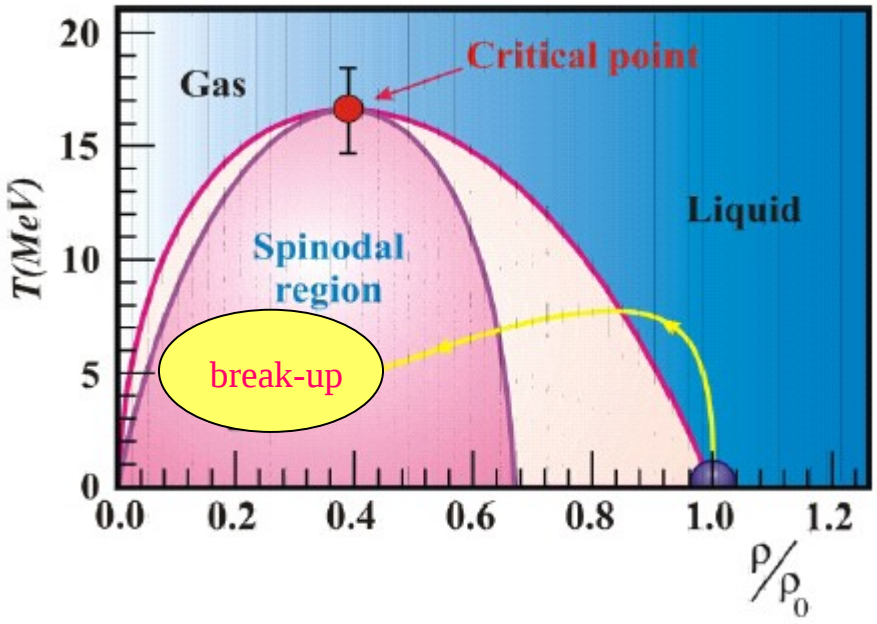

Statistical Multifragmentation Model (SMM)

J.P.Bondorf, A.S.Botvina, A.S.Iljinov, I.N.Mishustin, K.Sneppen, Phys. Rep. **257** (1995) 133

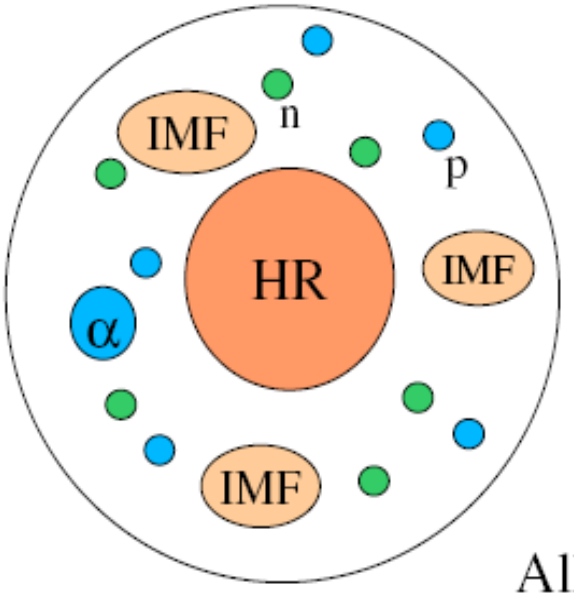

Ensemble of nucleons and fragments
in thermal equilibrium characterized by

neutron number N_0

proton number Z_0, $N_0+Z_0=A_0$

excitation energy $E^*=E_0-E_{CN}$

break-up volume $V=(1+\kappa)V_0$ freeze-out

All break-up channels are enumerated by the sets of fragment multiplicities or partitions, $f=\{N_{AZ}\}$

Statistical distribution of probabilities: $W_f \sim \exp\{S_f(A_0, Z_0, E^*, V)\}$
under conditions of baryon number (A), electric charge (Z) and energy (E*) conservation, including compound nucleus.

Production of large nuclear fragments in reaction initiated by high energy light particles and in peripheral nucleus-nucleus collisions:

Formation of excited nuclear residues (projectile/target) after the dynamical stage.

Multifragmentation in intermediate and high energy nuclear reactions

Experimentally established:

1) few stages of reactions leading to multifragmentation,
2) short time ~100fm/c for primary fragment production,
3) freeze-out density is around $0.1\rho_0$,
4) high degree of equilibration at the freeze-out,
5) primary fragments are hot.

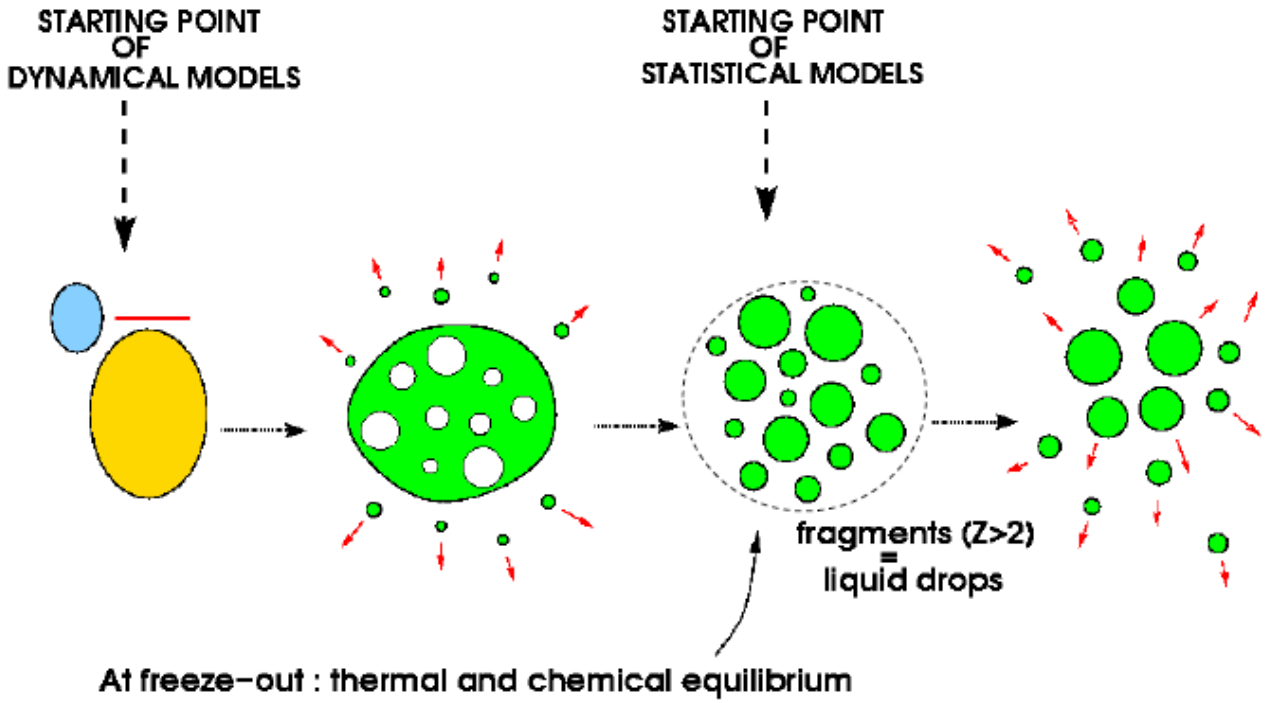

Two-stage multifragmentation of 1*A* GeV Kr, La, and Au

EOS collaboration: fragmentation of relativistic projectiles

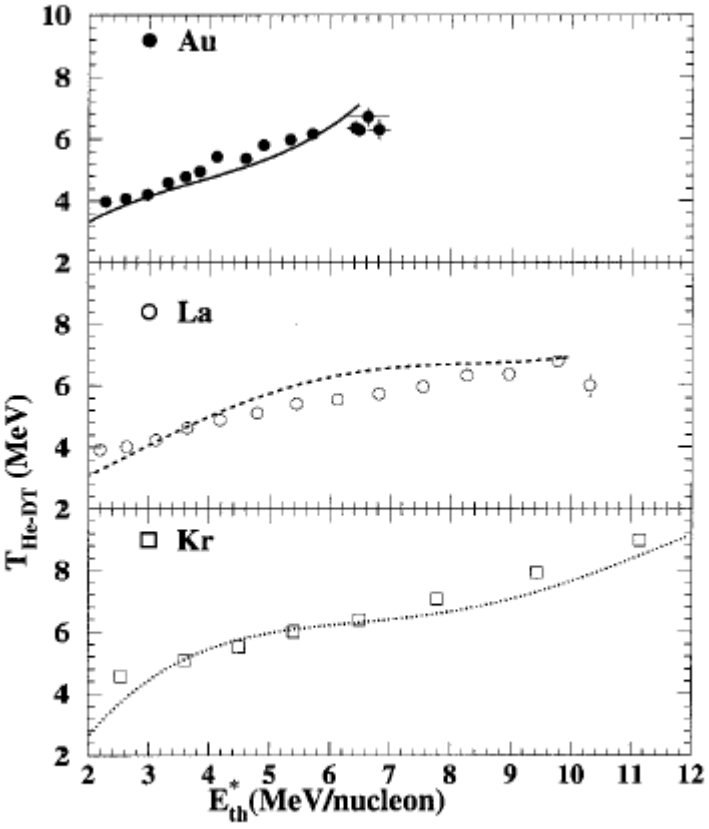

FIG. 19. Caloric curves (T_f vs E^*_{th}/A) for Kr, La, and Au. Points are experimental and curves are from SMM.

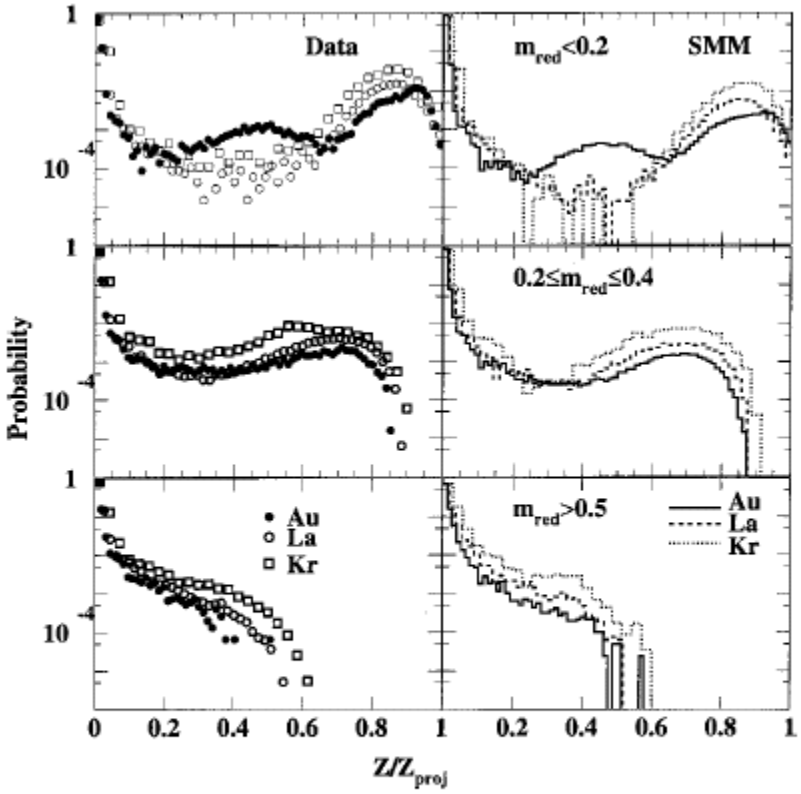

FIG. 24. Second stage fragment charge distribution as a function of $Z/Z_{\text{projectile}}$. Results are shown for three reduced multiplicity intervals for both data and SMM.

ALADIN data

GSI

multifragmentation of relativistic projectiles

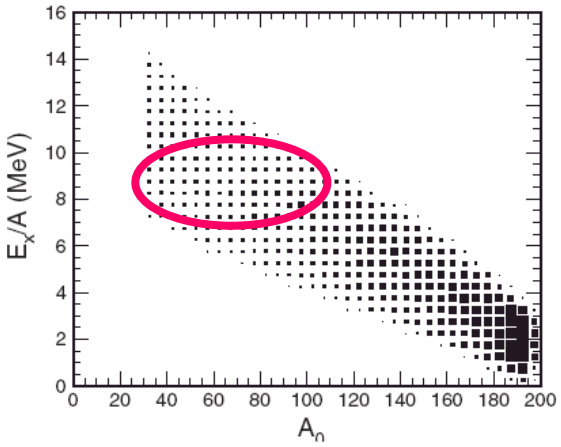

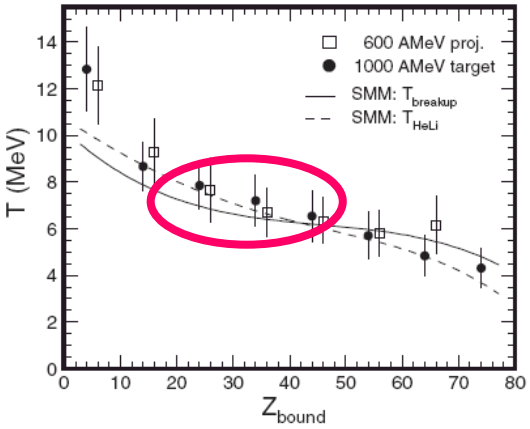

Au(600MeV/n)+C,Al,Cu

A.S.Botvina et al.,
Nucl.Phys. A584(1995)737

H.Xi et al.,
Z.Phys. A359(1997)397

comparison with SMM (statistical multifragmentation model)

Statistical equilibrium has been reached in these reactions

Au(600MeV/n)+Cu

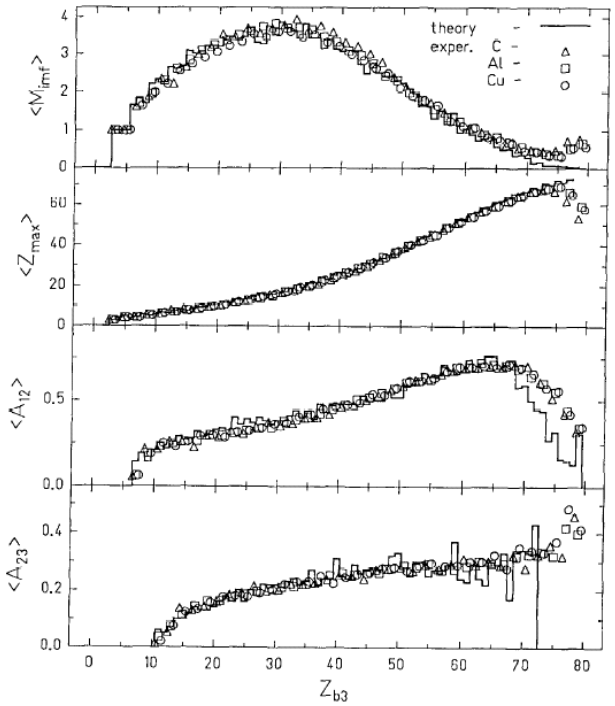

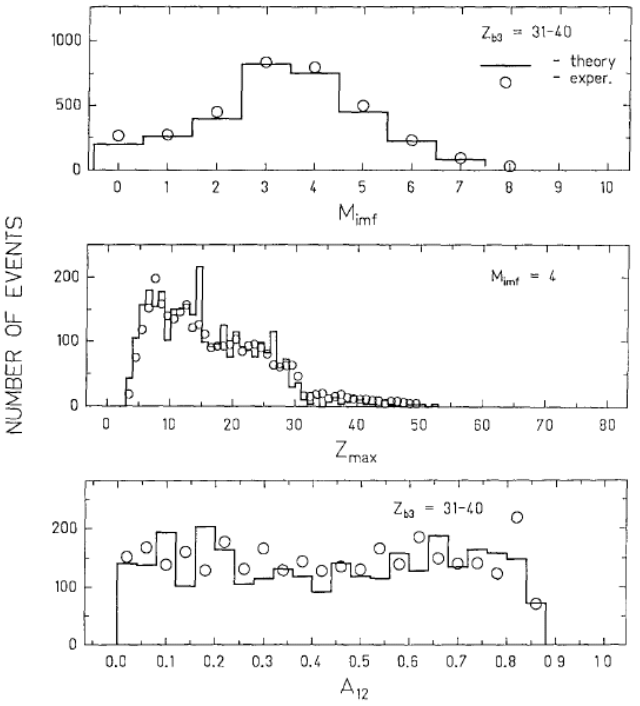

Formation of baryon clusters from the dynamically produced baryons as a results of secondary interaction between them, when they are in the vicinity of each other. Note: baryons in clusters can come to equilibrium and the clusters are excited respective to its ground state. This case is realized in Heavy- Ion collisions of medium/high energies.

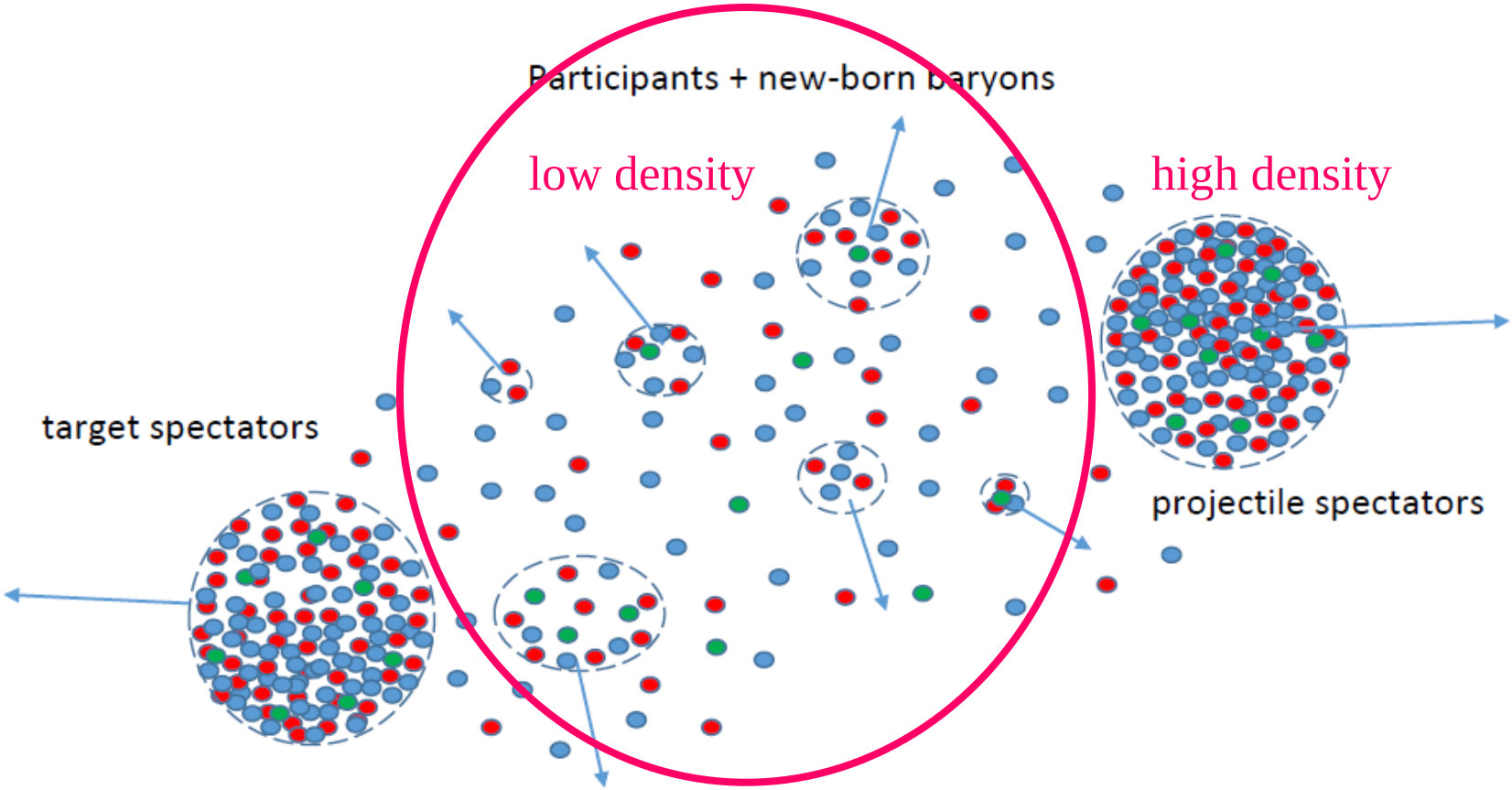

CENTRAL COLLISIONS: fast expansion of excited nuclear matter

Nuclear system expands to low densities and passes the density around 0.1 of normal nuclear density, which corresponds to the freeze-out adopted in the statistical models. Baryons can still interact and form nuclei at this density. We divide the nuclear matter into clusters in LOCAL chemical equilibrium and apply SMM to describe the nucleation process in these clusters.

dynamical expansion after collision/compress.

Baryonic clusters in local equilibrium (freeze-out)

nuclei formation inside the clusters - SMM

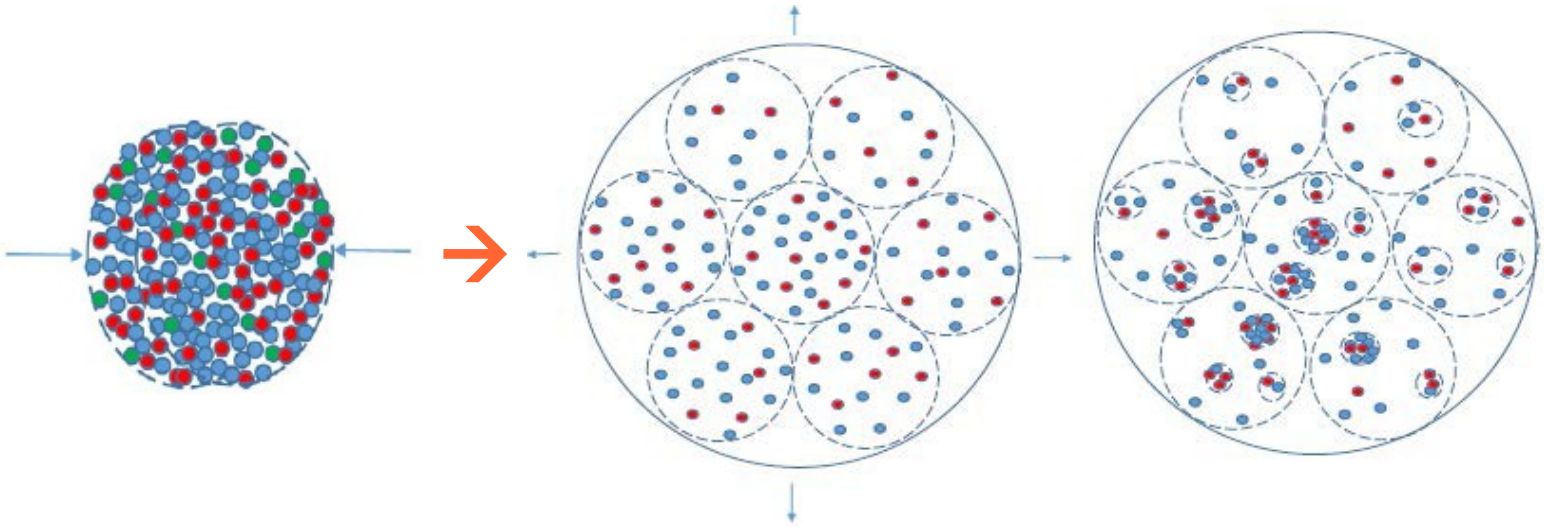

CENTRAL COLLISIONS: one can apply the special selection of events of nucleus-nucleus collisions (e.g., ERAT criterion in FOPI experiment). This selection can also require the special model application.

To describe this nuclei formation with controlled models:

Phys.Rev.C103 (2021) 064602 + Phys.Rev.C106 (2022) 014607

The dynamical stage is simulated with the phase space generation (PSG) and hydrodynamical-like generation (HYG) methods. They provide very different momenta distributions of baryons which cover the most important limits expected after this stage.

Selection of primary clusters (at low freeze-out density) by using the coalescence of baryon (CB) model (Phys. Lett. B742, 7 (2015)): according to their velocities $|Vi - V0| \le Vc$ and coordinates $|Xi - X0| \le Xc$.

Statistical formation of nuclei inside these clusters with SMM: de-excitation of the excited clusters. The excitation energy (or local temperature) of such clusters is important characteritics for the nuclear matter.

For the first, the consistent comparison with FOPI@GSI experimental data - Nucl. Phys. A848(2010)366 - on fragment production in central HI collisions is performed: Both charge yields and flow energies.
Phys.Rev.C103(2021)064602 and Phys.Rev.C106(2022)1014607

yields of nuclei in different reactions:

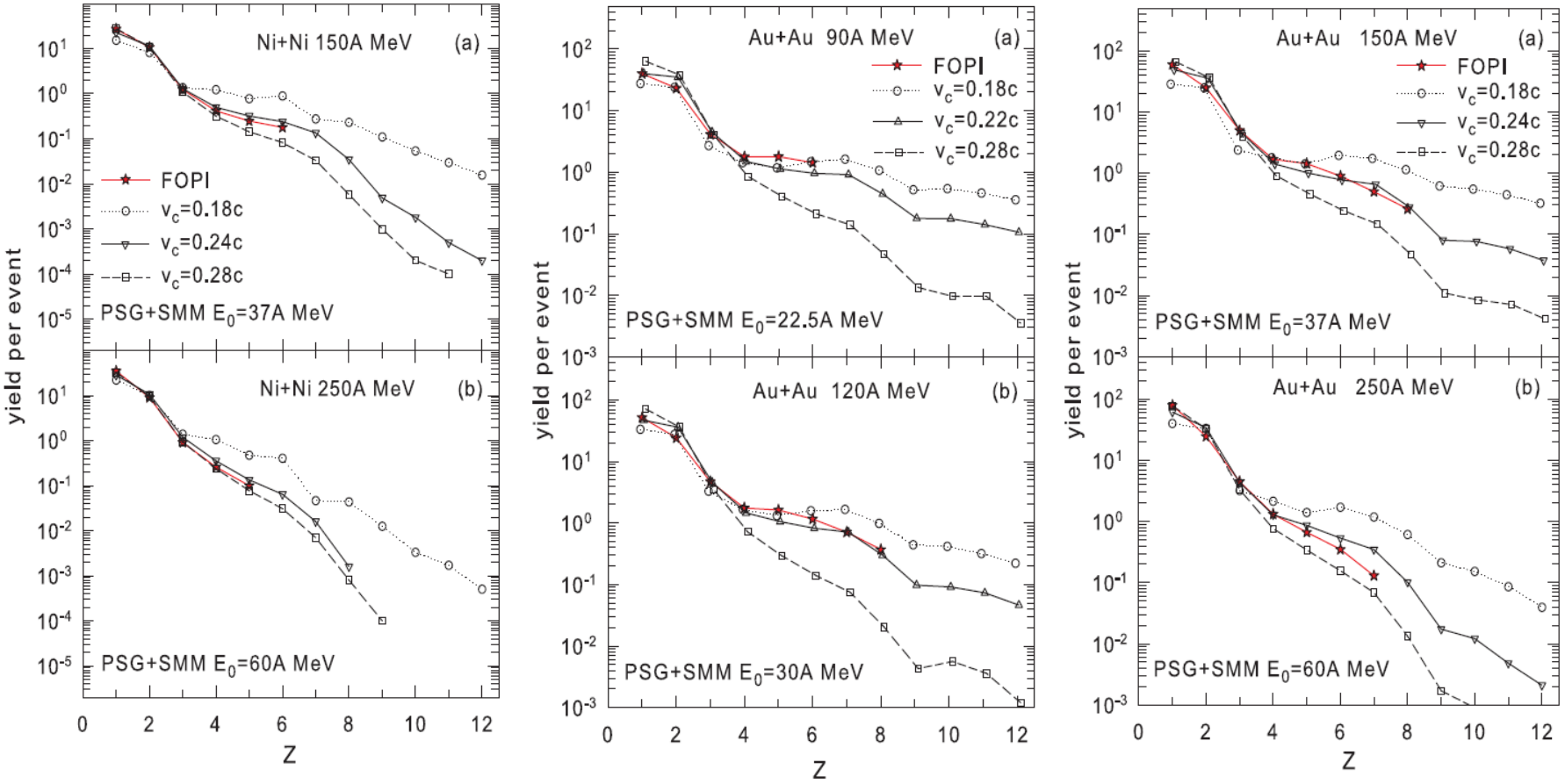

(until now the production of nuclei (Z>2) in central collisions was not possible to describe consistently)

kinetic energies of nuclei in different reactions:

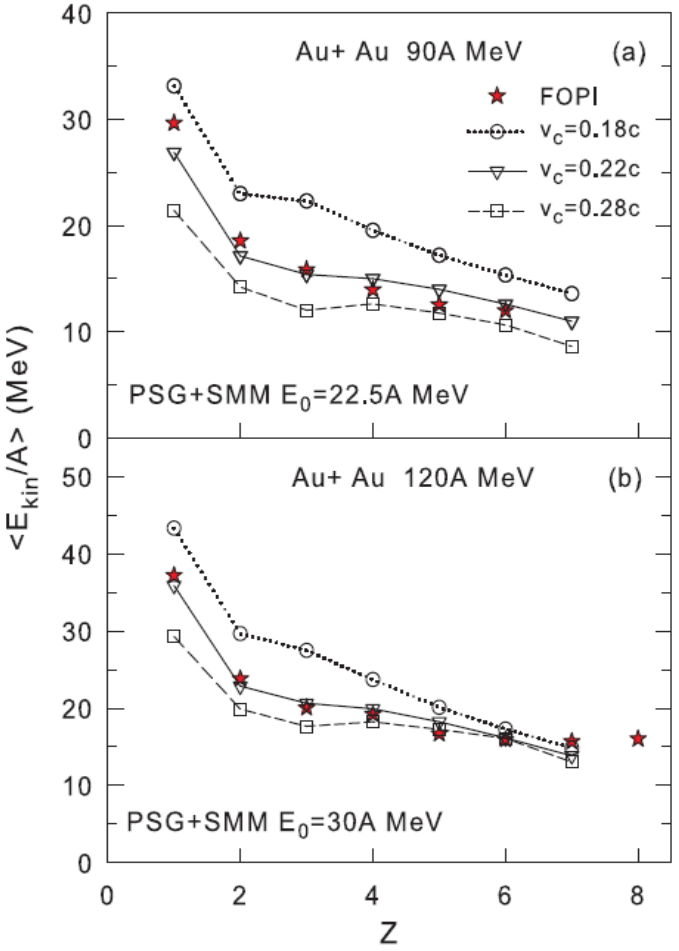

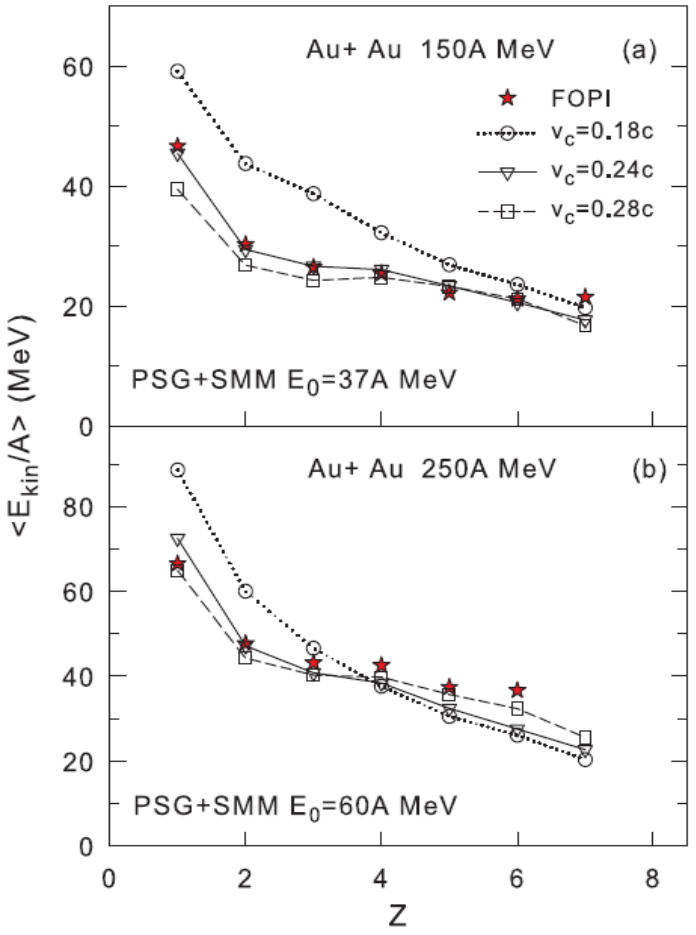

Important beam energy dependence of the light nuclei yields in Au+Au relativistic central collisions can be explained within our approach too.

Note: in simplistic coalescence picture yields of 3He are larger than 4He yields at all energies. FOPI experimental data (red symbols) show intersection with increasing energy.

Relative behavior of yields of 3He and 4He with energy is important confirmation of the nucleation via the statistical mechanism

Phys.Rev.C103 (2021) 064602

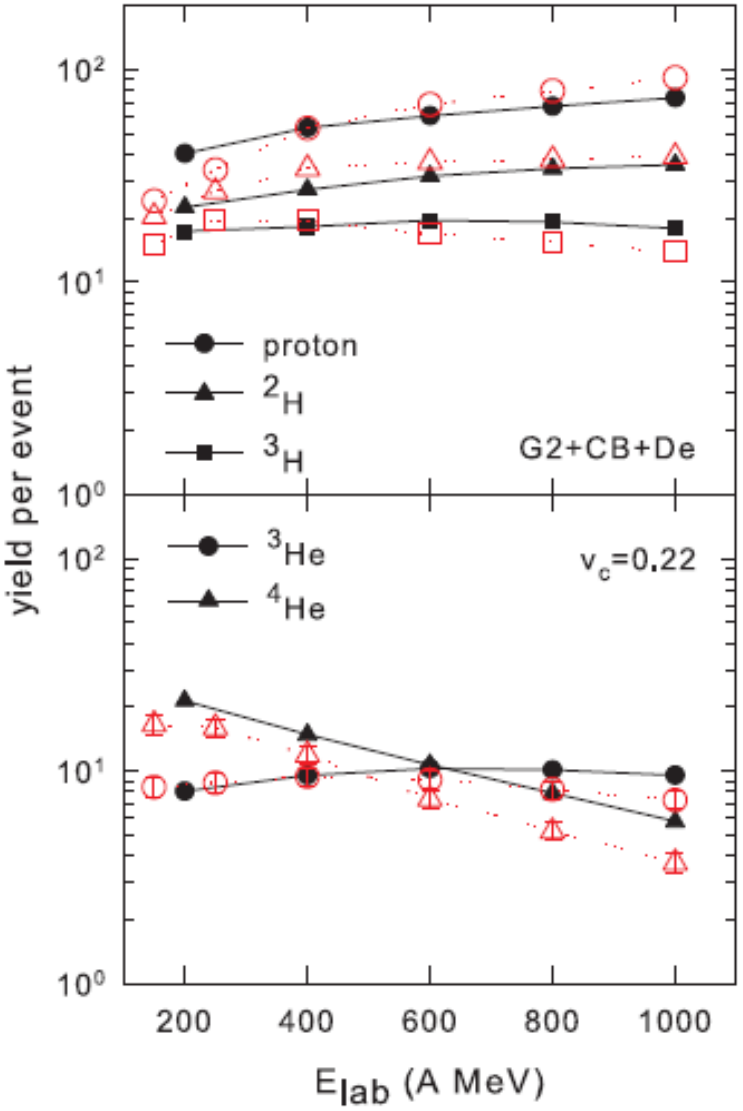

However, the description is possible if there is a limit for the excitation energy of the clusters: 6–10 MeV/nucleon, close to their binding energies. Temperature T=6--8 MeV (according to the statistical model) which corresponds to the coexistence region of the liquid-gas type phase transition in nuclear matter.

We may speak about an universal mechanism for nuclei formation both in peripheral and central heavy-ion collisions , independently on the way how the low density matter is produced: by thermal-like expansion of the excited residues (peripheral col.) or by dynamical-like expansion (central col.)

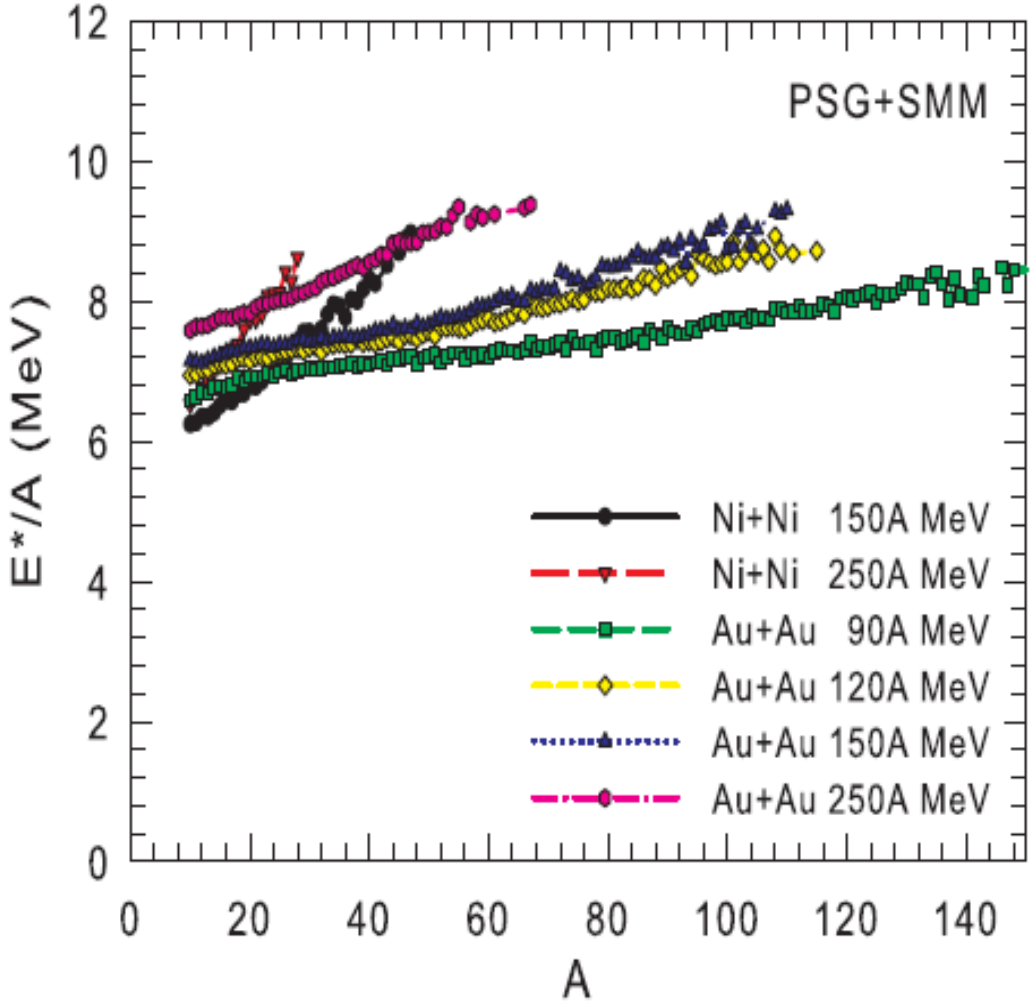

Conclusion on the nuclei production (disintegration of excited nuclei, or nucleation of individual baryons) described with the statistical approach:

Evolution of the statistical mechanism toward highly excited finite nuclear systems -

Compound nucleus conception –
excitation energies from 0 to 2-3 MeV/nucleon

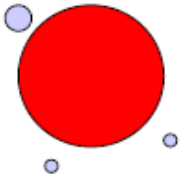

Freeze-out volume conception –
excitation energies from 2-3 to
8-10 MeV/nucleon

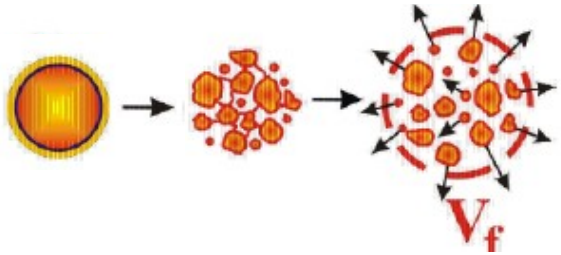

At energies more than 8-10 MeV/nucleon – fragmentation of the expanding nuclear matter at low density into locally equilibrated clusters with energies not higher than 8-10 MeV/nucleon and nucleation (nucleosynthesis) in such clusters

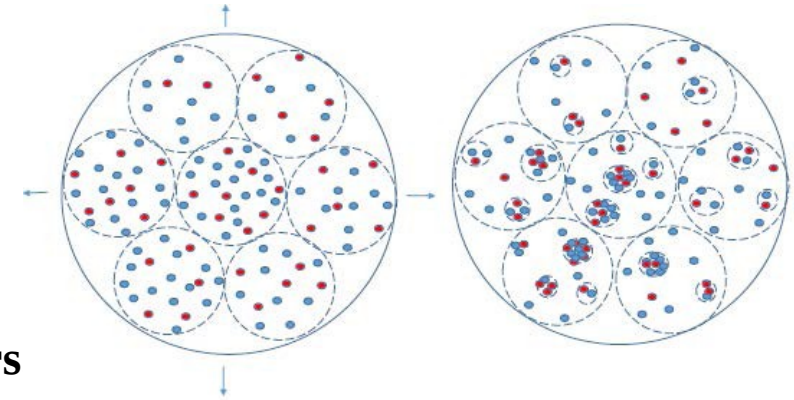

FAZIA experimental data [PRC**103**(2021)014603]: Peripheral collisions of 80-Kr with 40,48-Ca at 35 MeV/nucleon

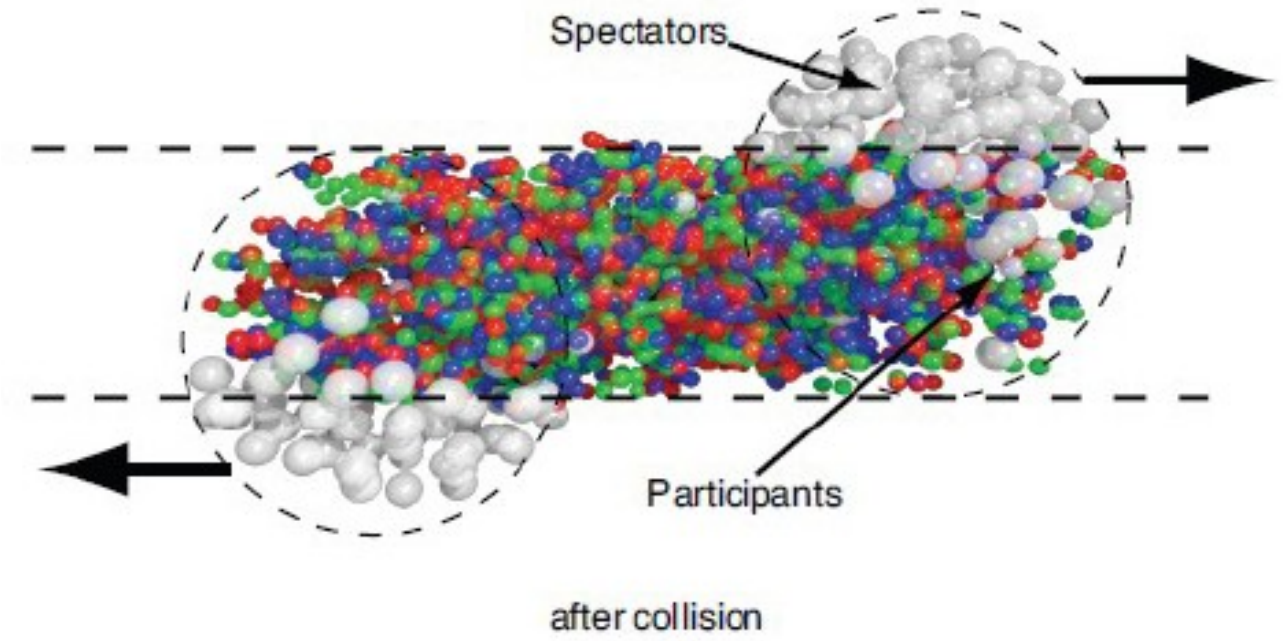

Fragments can be formed both in neck region (participant nucleons) and in spectator residue regions

R.Ogul et al., PRC107(2023)054606

We have suggested to describe FAZIA data with SMM by involving the ensemble of projectile sources (obtained after the dynamical stage) extracted previously for description of ALADIN data. The sources parameters are same (per nucleon), and this indicate an universal character of multifragmentation reaction in excited nuclear matter. Microcanonical description is important in the case of the phase space domination for small systems.

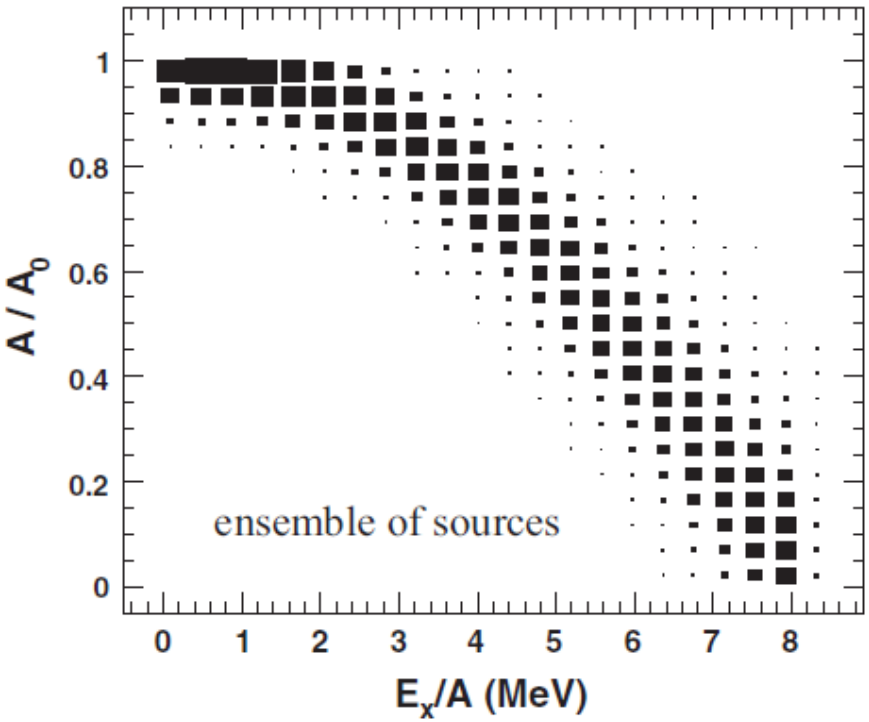

e.g., the predicted correlation: IMF and maximum fragment

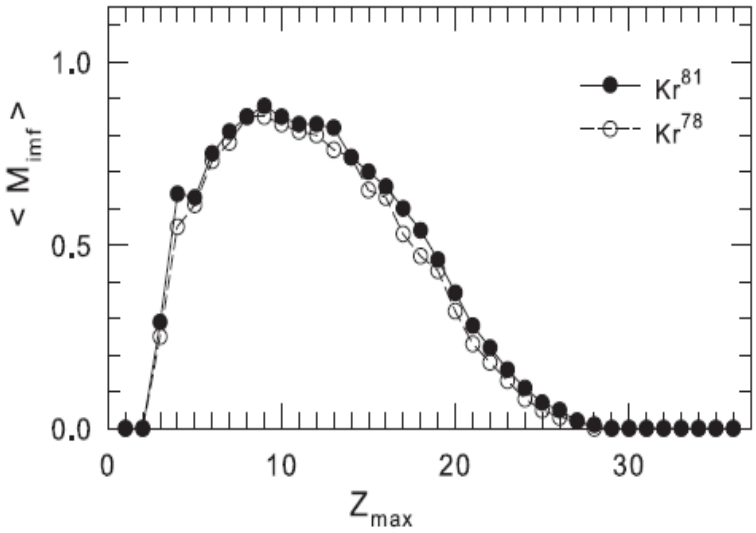

Isotope production of large projectile-like nuclei: SMM ensemble calculations and experimental data for peripheral collisions of 80-Kr with 40,48-Ca at 35 MeV/nucleon

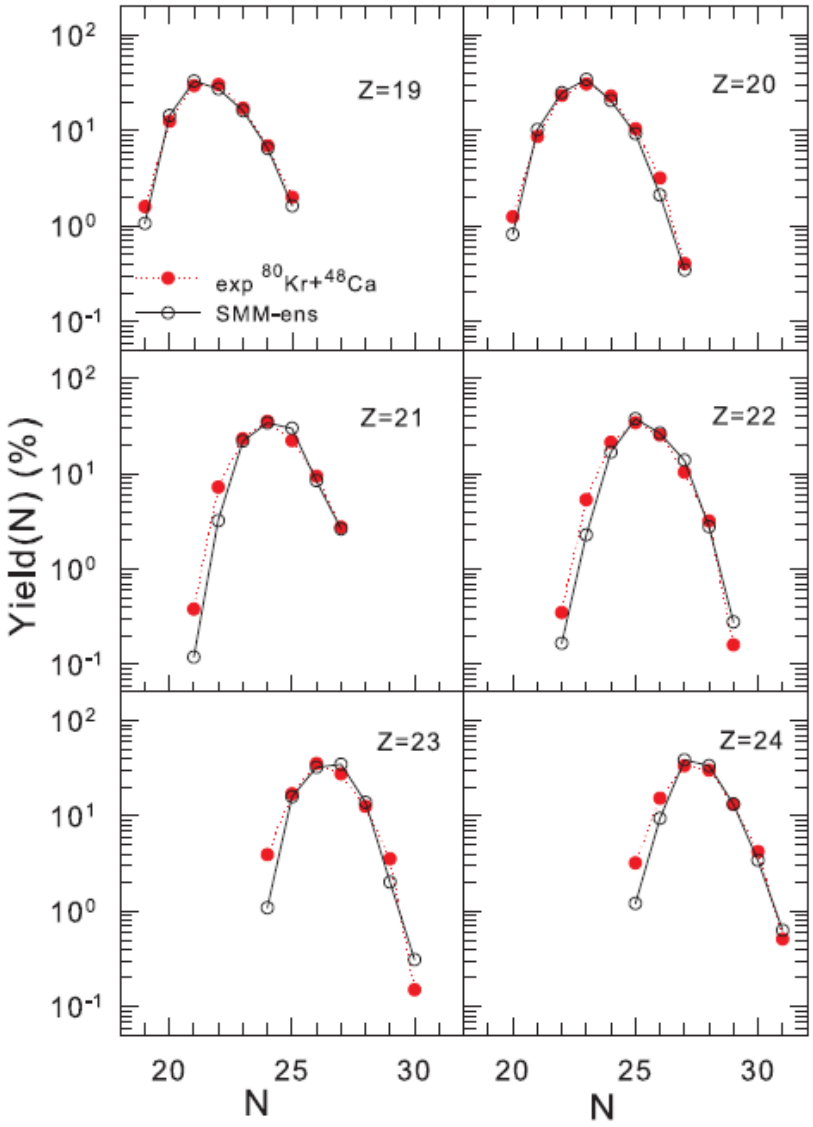

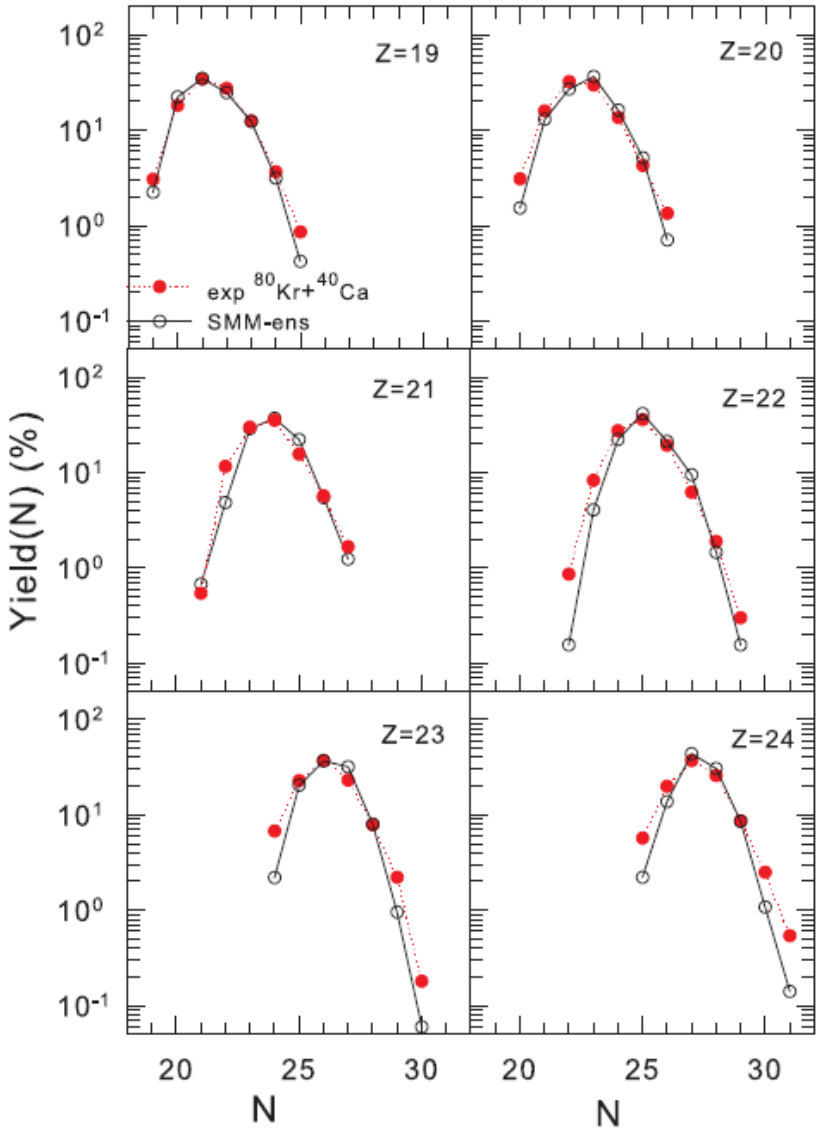

Yields of light nuclei correlated with the production of projectile fragments (forward emission).

Confirmation of SMM statistical calculations produced for the source ensemble.

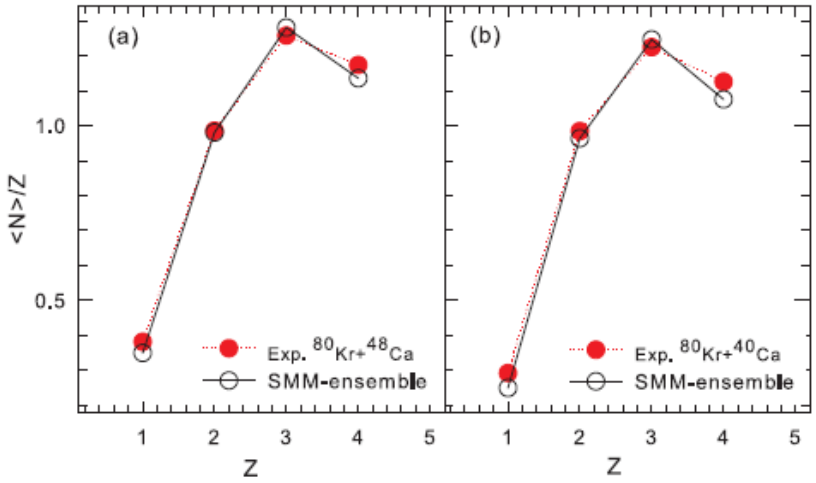

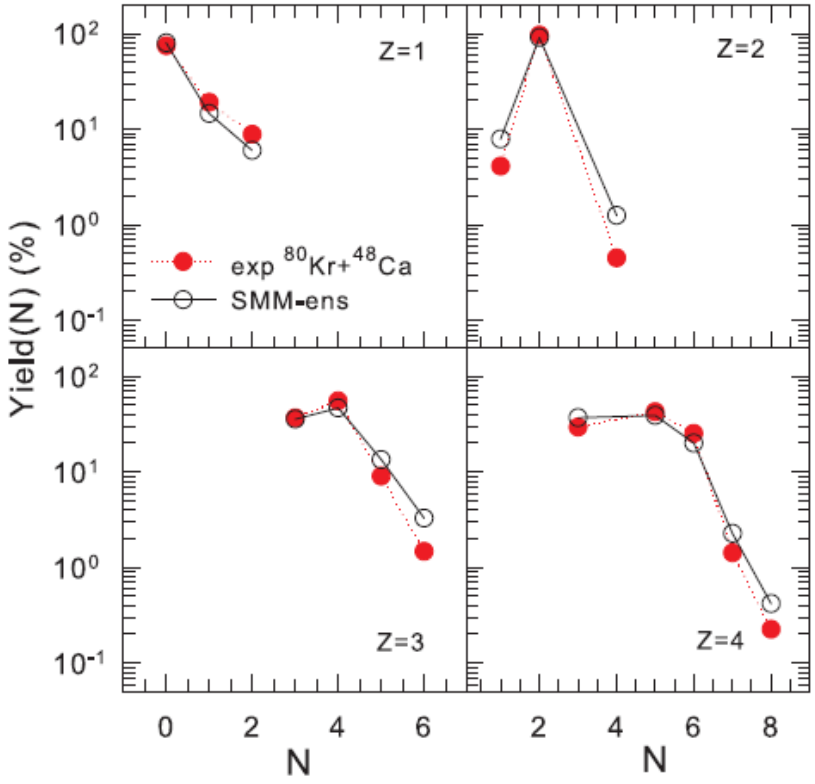

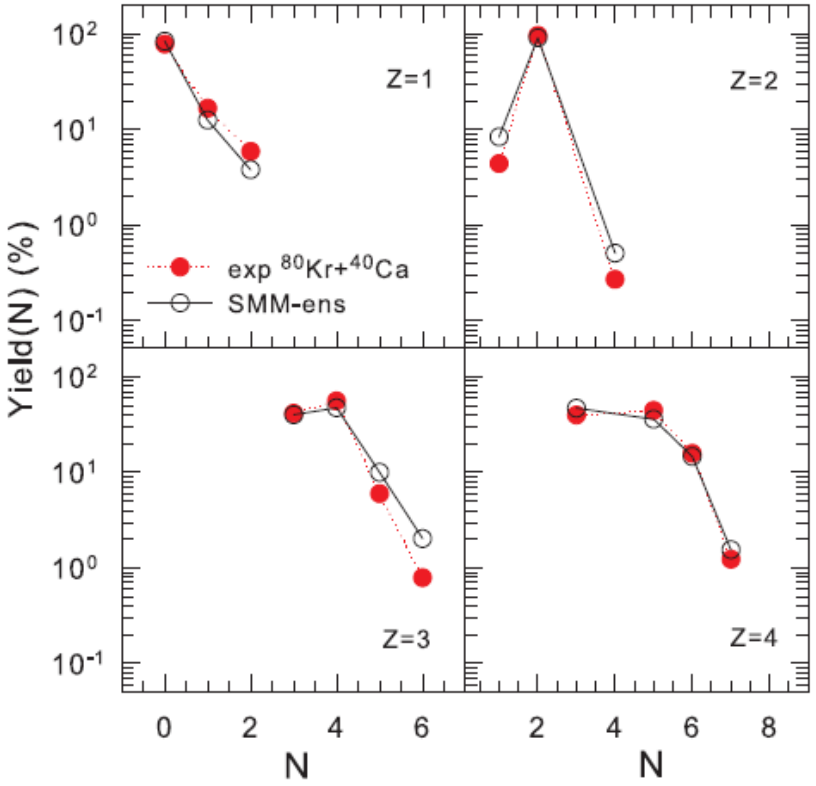

SMM-necklike emission: A low-density source of nucleons in local equilibrium (+correlated with the projectile/target-like sources) with A0=19, Z0=8, excitation E0=5 MeV/nucleon, density is 1/6 of normal nuclear one. The energy and density correspond to previous studies of multifragmentation in central collisions (Au+Au) at same beam energy of 35 MeV/nucleon. Local chemical equilibrium!

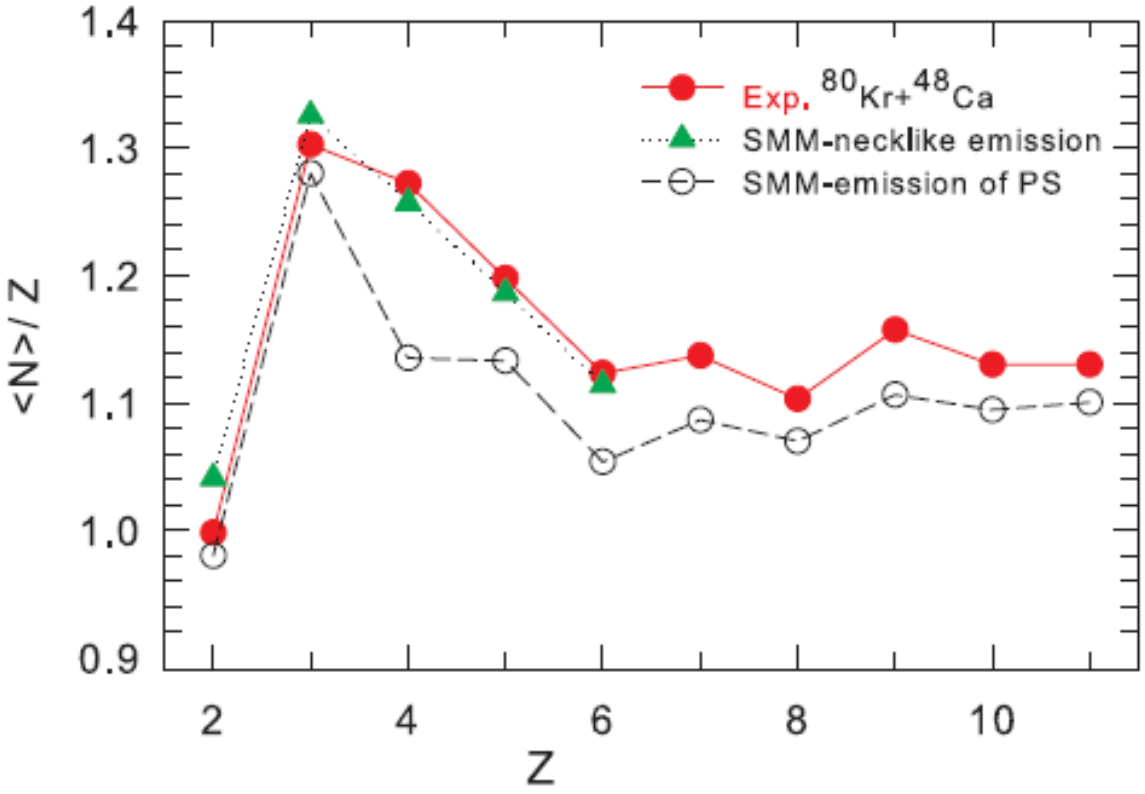

Physics Letters B 371 (1996) 175–180

Statistical multifragmentation in central Au + Au collisions at 35 MeV/u

MINIBALL + MULTICS

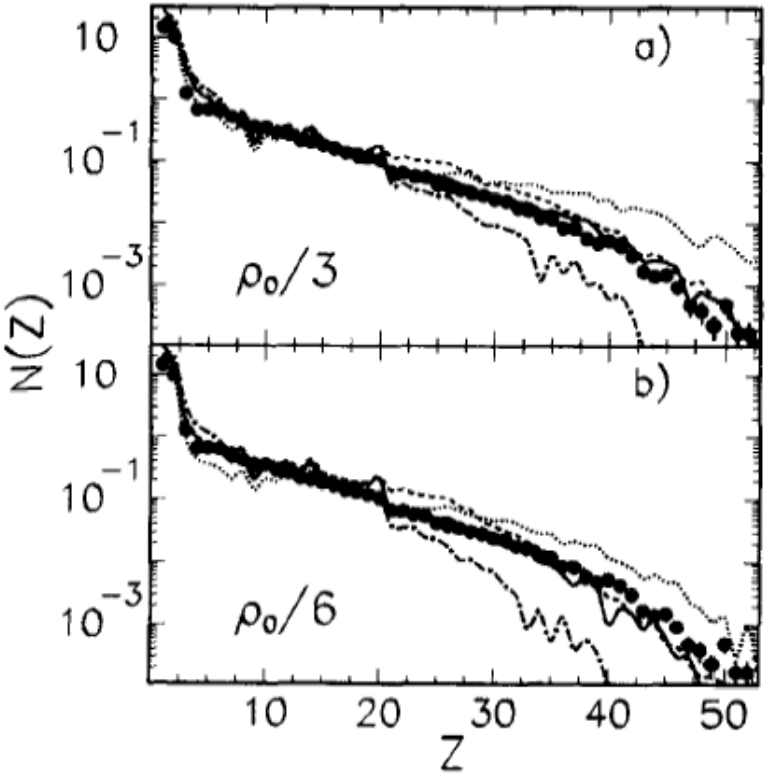

Fig. 1. Charge distribution $N(Z)$. Points show experimental data and lines show results of SMM predictions for sources with parameters $A_s = 343$, $Z_s = 138$, $E_s^*/A = 6.0$ MeV, $\rho_s = \rho_0/3$ (part a)) and $A_s = 315$, $Z_s = 126$, $E_s^*/A = 4.8$ MeV, $E_{flow}/A = 0.8$ MeV, $\rho_s = \rho_0/6$ (part b)). Dashed curves are the unfiltered calculations and solid curves are the filtered ones. The dot-dashed and dotted curves represent filtered calculations for thermal excitations $E_s^*/A + 1$ MeV/u and $E_s^*/A - 1$ MeV/u, respectively.

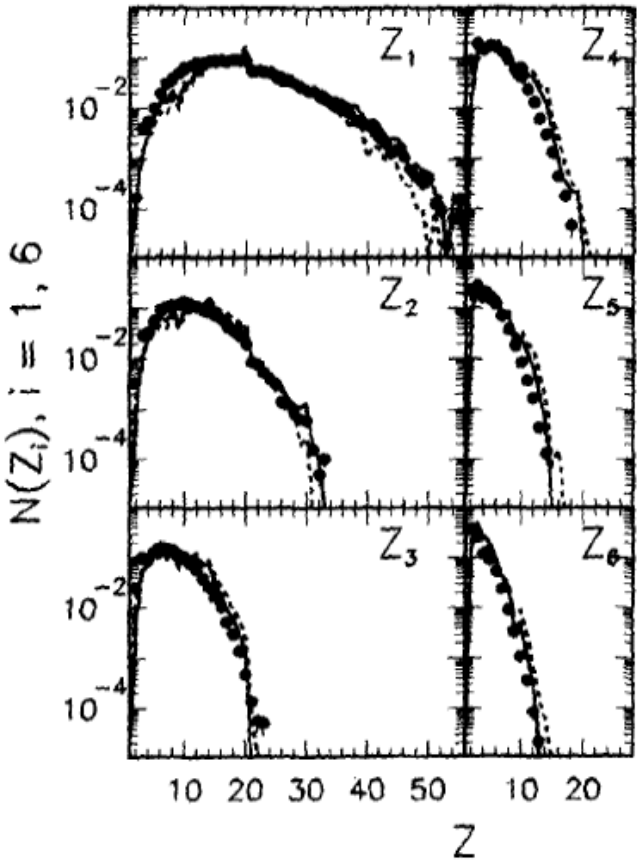

Fig. 2. Charge distribution of the six heaviest fragments, ordered such as $Z_i \geq Z_k$ if $i < k$. Experimental data are shown by points, the solid and dashed curves show the results of SMM calculations for $\rho_s = \rho_0/3$, and $\rho_s = \rho_0/6$, respectively (other source parameters as in Fig. 1).

Statistical description of supernova matter

Statistical ensemble
with fixed T, ρ_B, $Y_{L(e)}$

nuclear species (A,Z): $\boldsymbol{\mu_{AZ}} = A\boldsymbol{\mu} + Z\boldsymbol{\xi}$

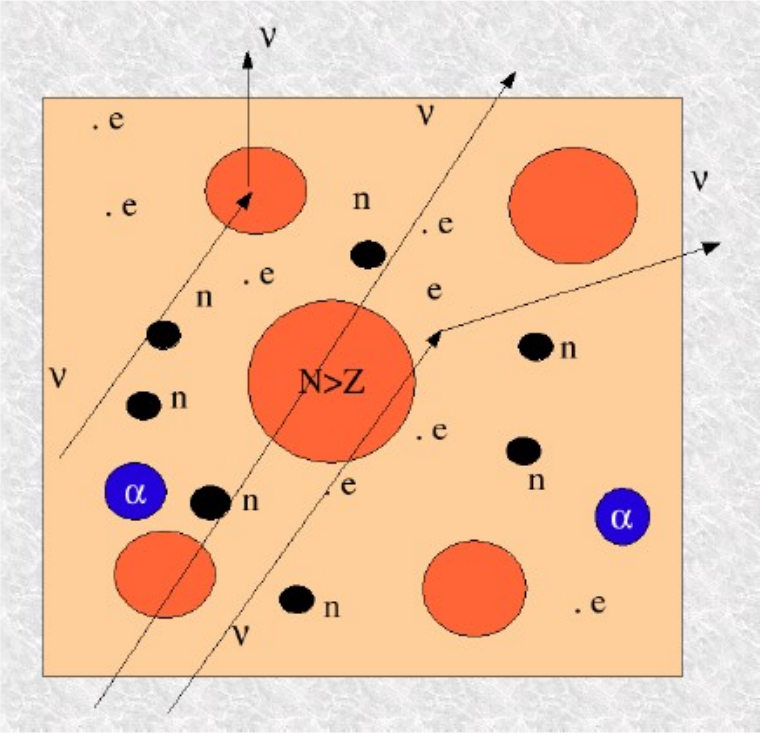

calculations done in a box
containing 1000 baryons

baryon number conservation

$$\rho_B = \Sigma_{AZ}\, A\, \rho_{AZ} \quad \text{find} \quad \boldsymbol{\mu}$$

electric neutrality

$$\rho_e = \Sigma_{AZ}\, Z\, \rho_{AZ} \quad \text{find} \quad \boldsymbol{\xi}$$

lepton number conservation

$$Y_L = \rho_e / \rho_B \quad (\text{free neutrinos})$$

$$Y_L = (\rho_e + \rho_\nu) / \rho_B \quad (\text{trapped } \nu)$$

A.S.Botvina and I.N.Mishustin, Phys.Lett. B584, 233 (2004);
Phys.Rev. C72, 048801 (2005)

Energy evolution of mass distributions of fragments in multifragmentation reactions and in stellar mater

A.S. Botvina, I.N. Mishustin / Nuclear Physics A 843 (2010) 98–132

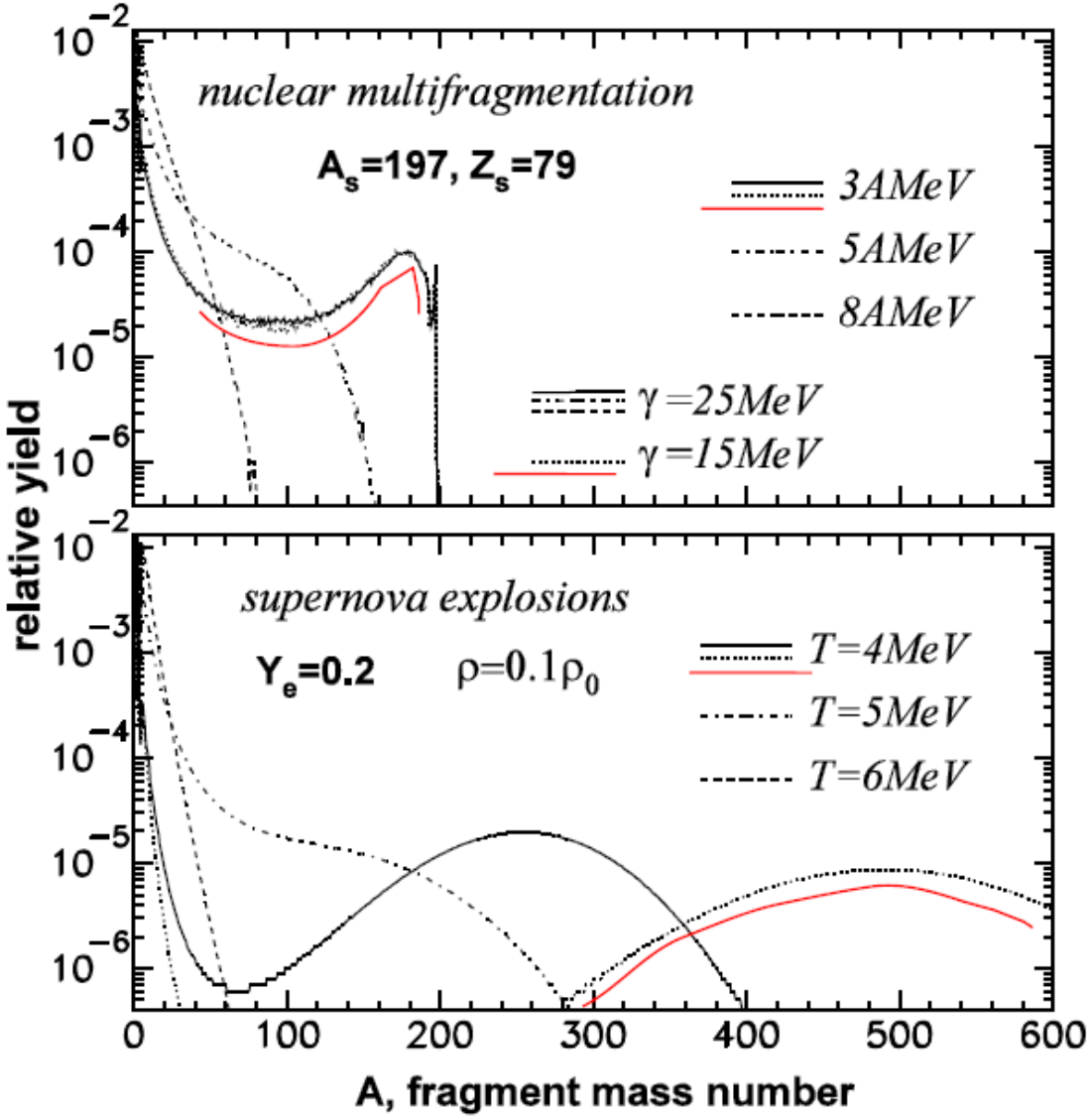

R.Ogul et al. PRC **83,** 024608 (2011) **ALADIN@GSI**

Isospin-dependent multifragmentation of relativistic projectiles

124,107-**Sn**, 124-**La** (600 A MeV) + **Sn** → projectile (multi-)fragmentation

Very good description is obtained within Statistical Multifragmentation Model, including fragment charge yields, isotope yileds, various fragment correlations.

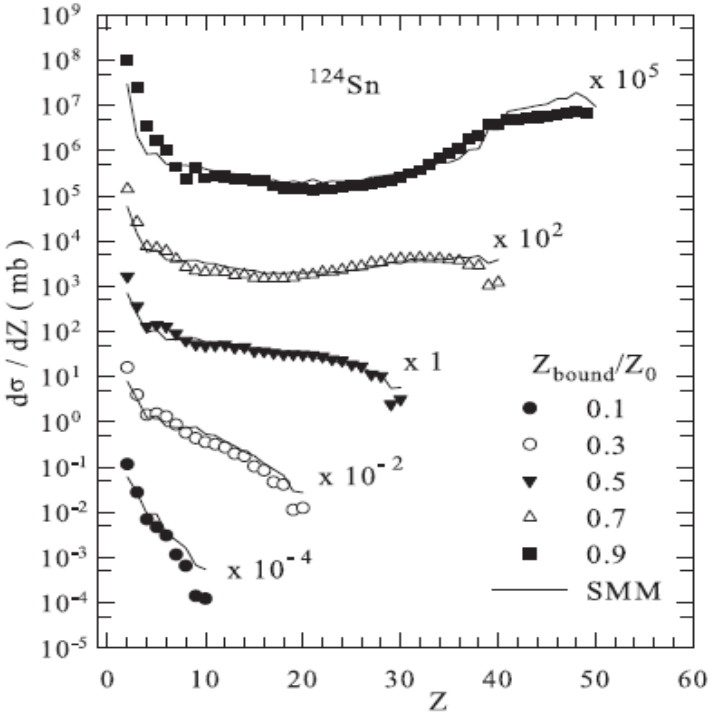

Statistical (chemical) equilibrium is established at break-up of hot projectile residues ! In the case of strangeness admixture we expect it too !

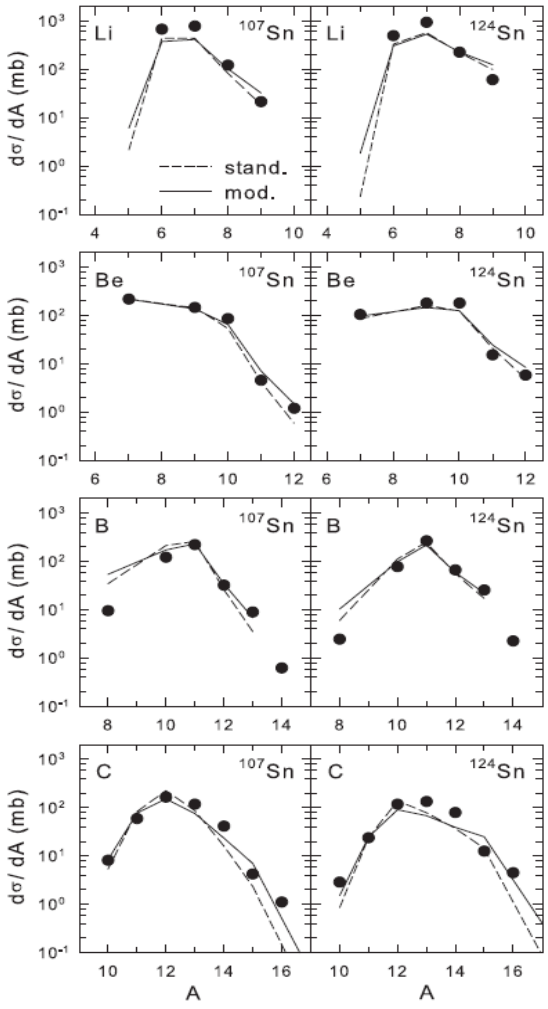

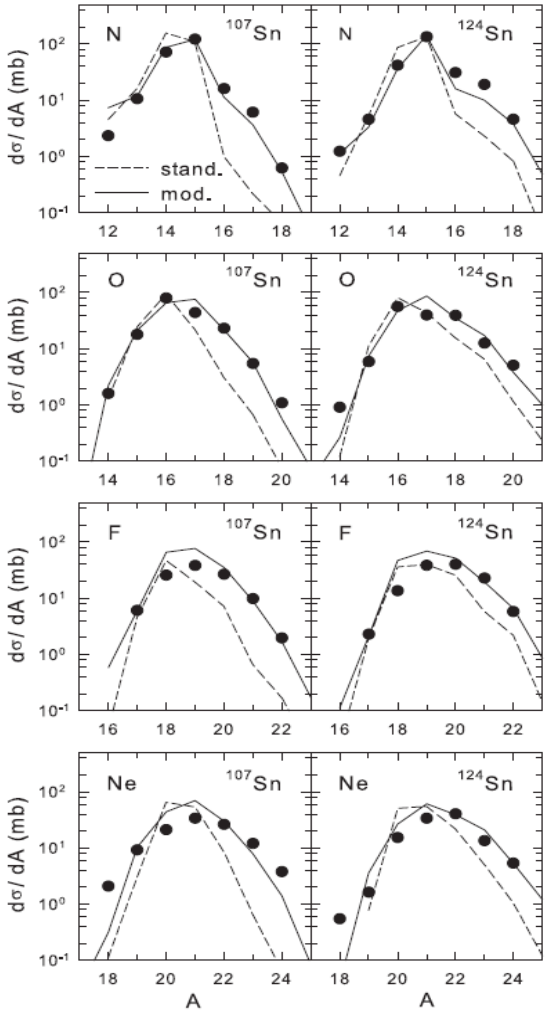

Electro-weak processes:

electron capture rates, R_e (per nucleon, per second)

using K.Langanke et al. Phys.Rev.Lett. 90, 241102 (2003)

Independent particle model, Gamow-Teller transitions dominate

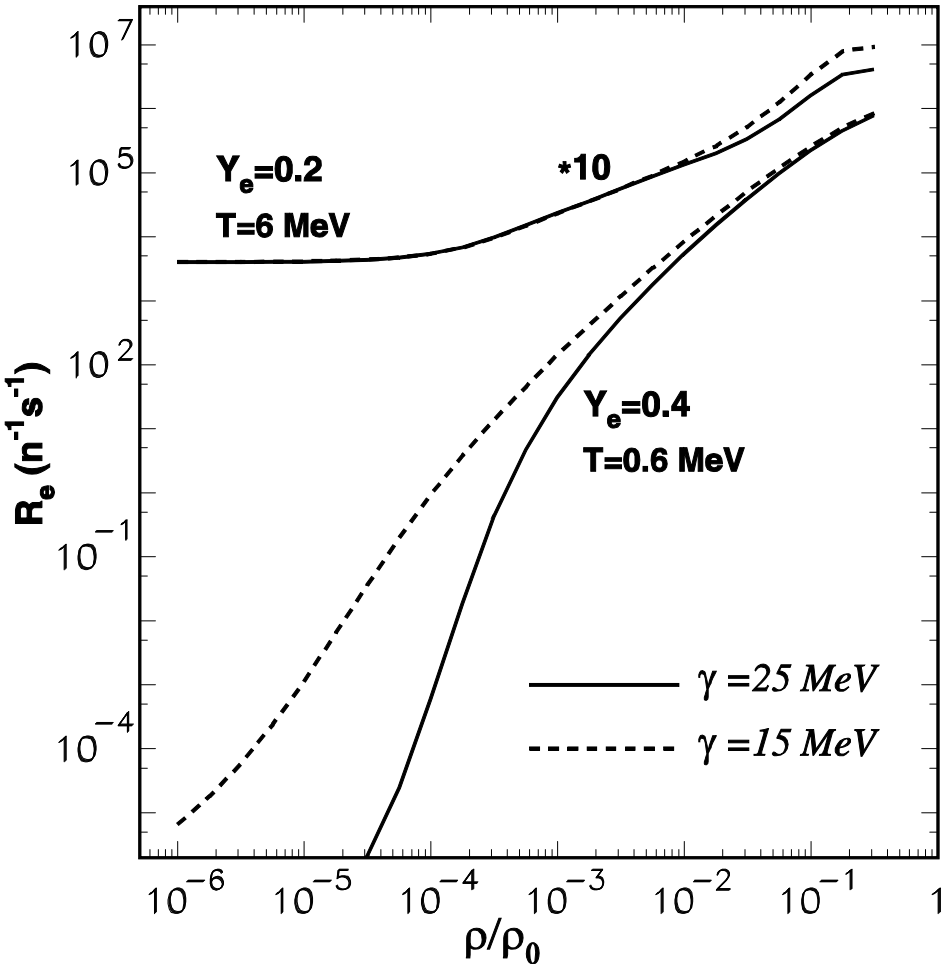

dependence on
the symmetry energy
of nuclei

$E_{sym}=\gamma(A-2Z)^2/A$

Conclusions

Collisions of energetic ions do lead to the nucleosynthesis of nuclei, including exotic species. These processes can be simulated within dynamical and statistical models.

Mechanisms for the formation of the nuclei in reactions: 1) de-excitation of the spectator matter, 2) nucleation of the produced particles at subnuclear density. The last one leads to light miclei and is effective at all rapidities.
Novel mechanism: The expanded matter is subdivided into excited baryon clusters in local equilibrium, and after the cluster decay the nuclei of all sizes (and isospin), including short-lived weakly-bound states, multi-strange nuclei can be produced. Microcanonical statistical description works for such correlated local sources!

There is no limit on sizes and isotope content of produced exotic nuclei; probability of their formation may be high; a large strangeness can be deposited in nuclei.
EOS/properties of nuclear matter can be addressed via the fragment formation:
In particular, symmetry energy of fragments formed at the subnuclear densities can be extracted.
Correlations (unbound states) and lifetimes can be naturally studied.

MINIBALL + MULTICS

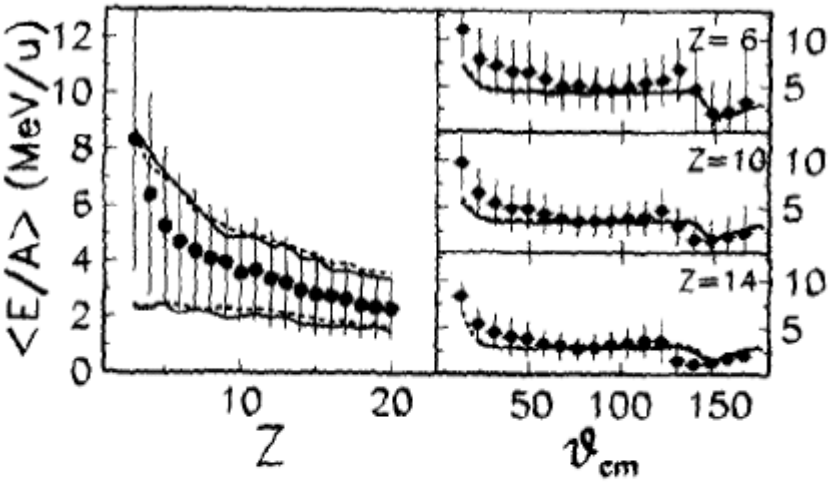

Fig. 3. Mean centre-of-mass kinetic energy per nucleon, $\langle E/A \rangle$, as a function of the charge Z, for fragments emitted at $\theta_{cm} = 90° \pm 10°$ (left panel) and (for $Z = 6, 10, 14$) as a function of θ_{cm} (right panels). Points give the experimental values of $\langle E/A \rangle$ and vertical bars give the standard deviations $\Delta E/A$ of the distributions. The solid and dashed lines are SMM predictions of $\langle E/A \rangle$ (in the left panel show the two values $\langle E/A \rangle \pm \Delta E/A$) for $\rho_s = \rho_0/3$, and $\rho_s = \rho_0/6$, respectively (other source parameters as in Fig. 1). The energy range is the same in the left and in each right panel.

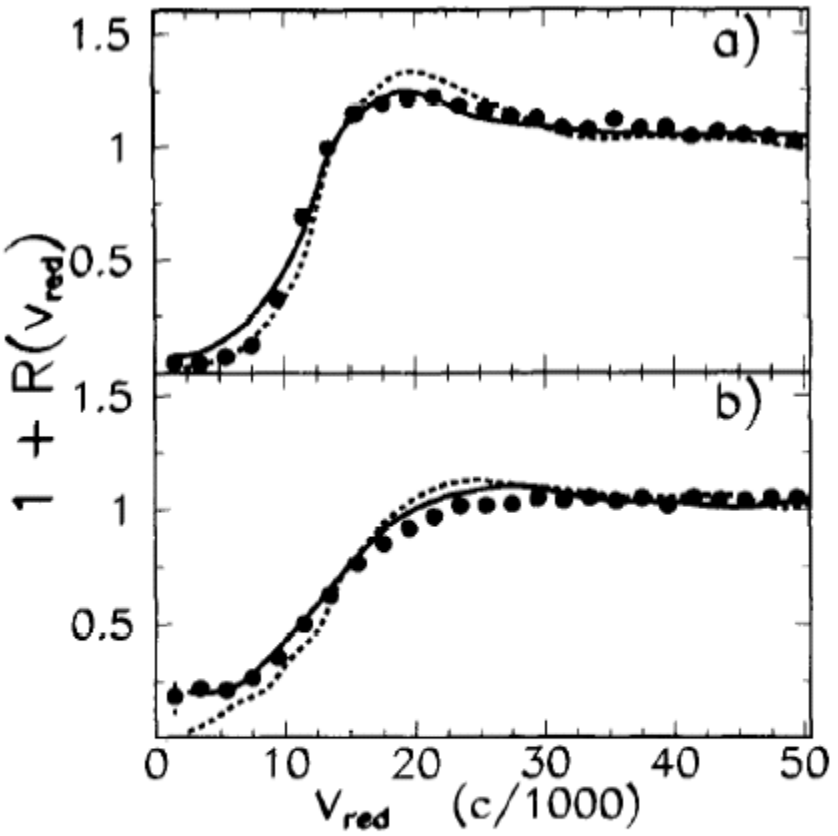

Fig. 4. Two-fragment correlation functions $1 + R(v_{red})$ for $3 \leq Z \leq 30$ and $8° \leq \theta_{lab} < 23°$ (part a)) and for $3 \leq Z \leq 10$ and $23° \leq \theta_{lab} \leq 40°$ (part b)). Full points show experimental data. The solid and dashed lines are SMM predictions for $\rho_s = \rho_0/3$, and $\rho_s = \rho_0/6$ (other source parameters as in Fig. 1).

UrQMD PHSD DCM GiBUU

Production mechanisms of nuclear cluster species including anti-matter, hyper-matter in relativistic HI and hadron collisions:

- Production of all kind of particles (anti- , strange, charmed ones) in individual binary hadron collisions. Effects of nuclear medium can be included.
- Secondary interactions and rescattering of new-born particles are taken into account. (Looks as partial ‘thermalization’.)
- Nucleation process of produced baryons into composite (normal. exotic, anti- , hyper-) nuclear species.
- Capture of produced baryons by big excited nuclear residues.

Statistical decay of excited nuclear species into final nuclei

- Multifragmentation into small nuclei (high excitations),
- Evaporation and fission of large nuclei (low excitations),
- (Fermi-) Break-up of small nuclei into lightest ones.

Multifragmentation versus sequential evaporation

ISIS π^-(8GeV/c)+Au

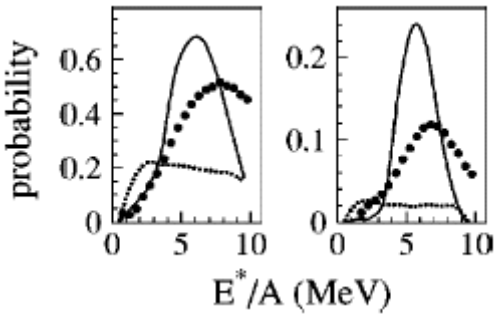

FIG. 3. Left panel: dots present the raw measured probability to detect an event with at least one heavy-fragment, $Z \geqslant 8$, and solid (dotted) line presents the SMM (GEMINI) model prediction filtered with the experimental detection efficiency. An initial angular momentum of $L = 20\hbar$ for the hot nucleus was assumed for GEMINI model calculations. Right panel: as in left panel, but for the probability of detecting events with at least two heavy-fragments, $Z \geqslant 8$.

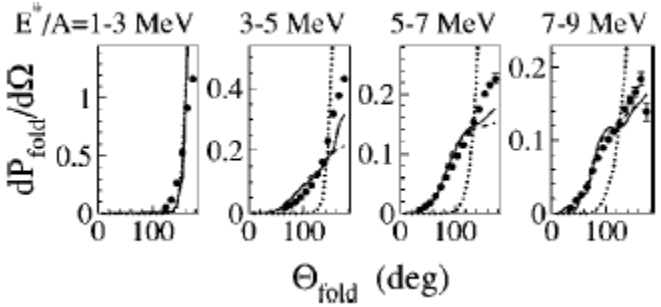

FIG. 2. The measured folding-angle (the angle between two $Z \geqslant 8$ fragments) probability for the indicated excitation-energy bins. Solid, dashed, and dotted lines show the SMM-hot, SMM-cold, and GEMINI model predictions, respectively, filtered with the experimental detection efficiency.

ALADIN Au (600 MeV/n) +X.

Nuclear Physics A556 (1993) 672–696

P. Kreutz et al. / Charge correlations

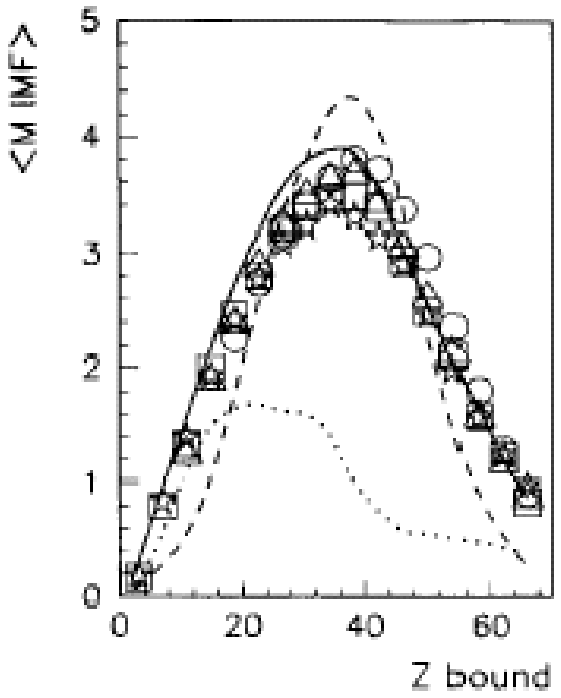

Fig. 15. The average multiplicity of IMFs as a function of Z_{bound} for Au 600 MeV/nucleon collisions on C (circles), Al (triangles), Cu (squares) and Pb (stars). The error bars are in most cases smaller than the size of the symbols. The lines are COPENHAGEN (dashed), GEMINI (dotted) and percolation (full) predictions.

Time scale of the thermal multifragmentation

FASA

collaboration

angle correlations of fragments

p(8.1 GeV) + Au

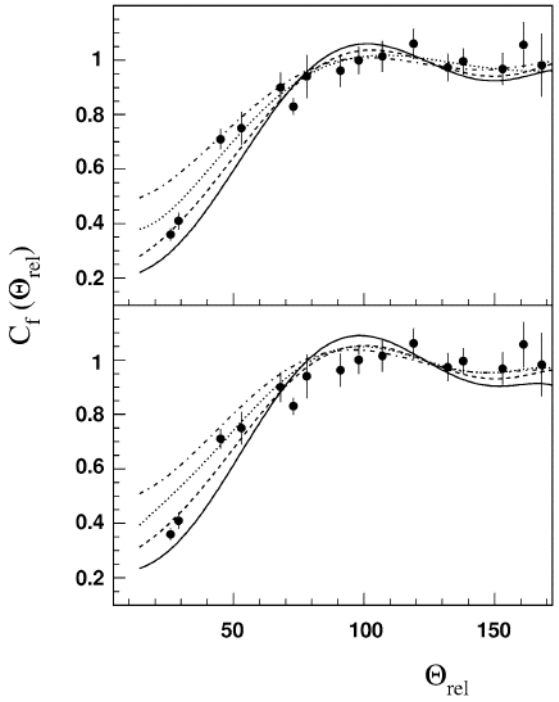

Fig. 5. Comparison of the measured correlation functions (full circles) with the calculated ones for different mean decay times of the fragmenting system: solid, dashed, dotted and dash-dotted lines for $\tau = 0$, 50, 100 and 200 fm/c. The upper panel is for the RC + α + SMM model with the parameters $(4, 8, \eta)$ (see notation in Fig. 4), the lower panel is for the same model, but with the parameters $(4, 4, \eta)$ allowing the fragments to overlap (see text).

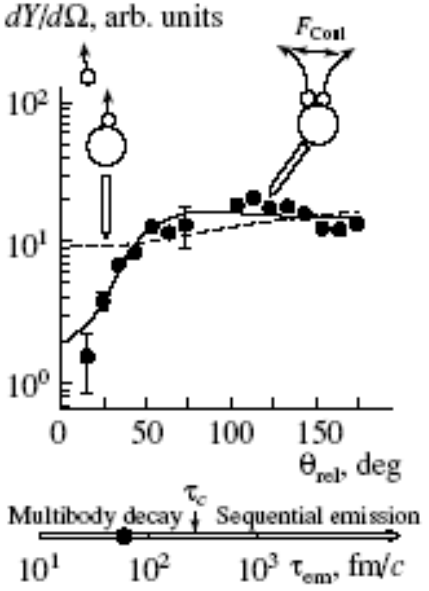

Fig. 5. Distribution of relative angles between coincident IMFs for ^{4}He(14.6 GeV) + Au collisions. The solid curve is calculated for the simultaneous emission of fragments; the dashed curve corresponds to the sequential, independent evaporation.

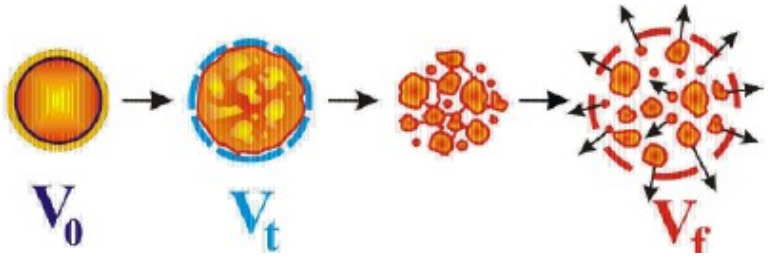

Time scale of the thermal multifragmentation

ISIS collaboration

velocity correlations of fragments

π^-(8GeV/c)+Au

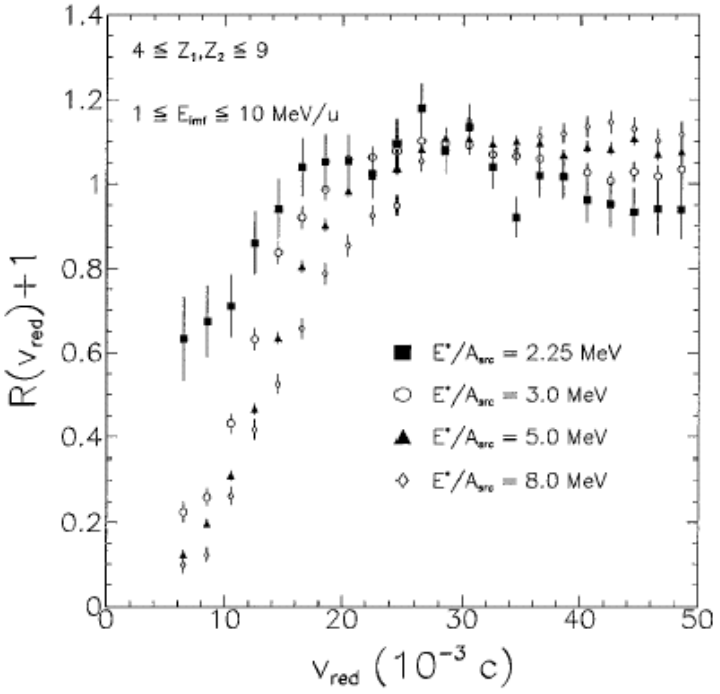

FIG. 1. Reduced velocity correlation functions generated for four different excitation energy per nucleon bins. IMF kinetic energy acceptance is in source frame is $E_{\mathrm{IMF}}/A = 1-10$ MeV.

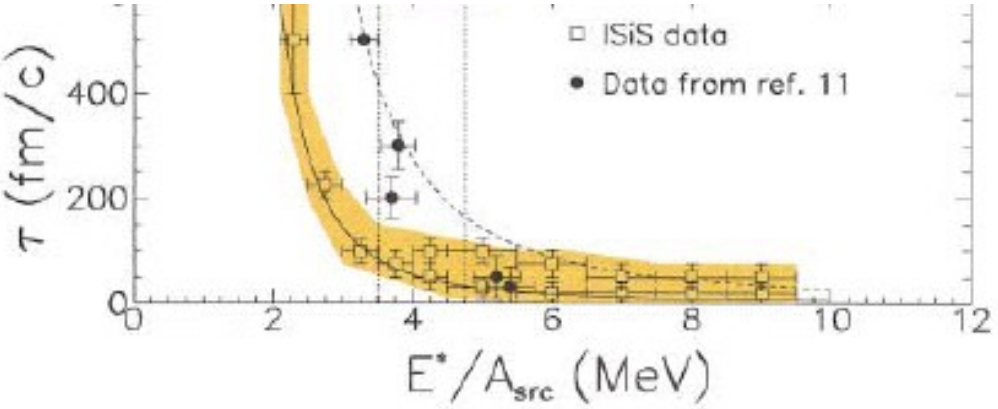

L.Beaulieu et al., Phys. Rev. Lett. **84**, 5971 (2000)

Excitation energies of the nuclear spectator residuals

DCM : PRC95, 014902 (2017)

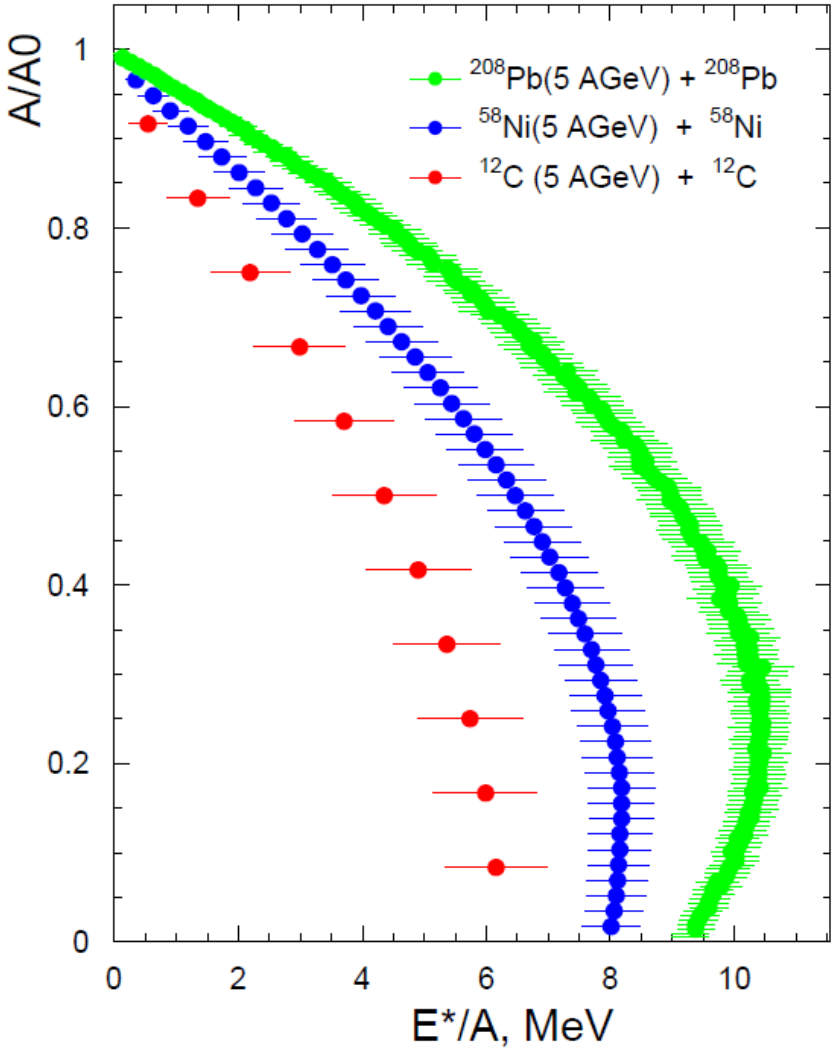

PRC84, 064904 (2011)

Masses of projectile residuals produced at dynamical stage (6b: H=0, 0.2b: H>0)

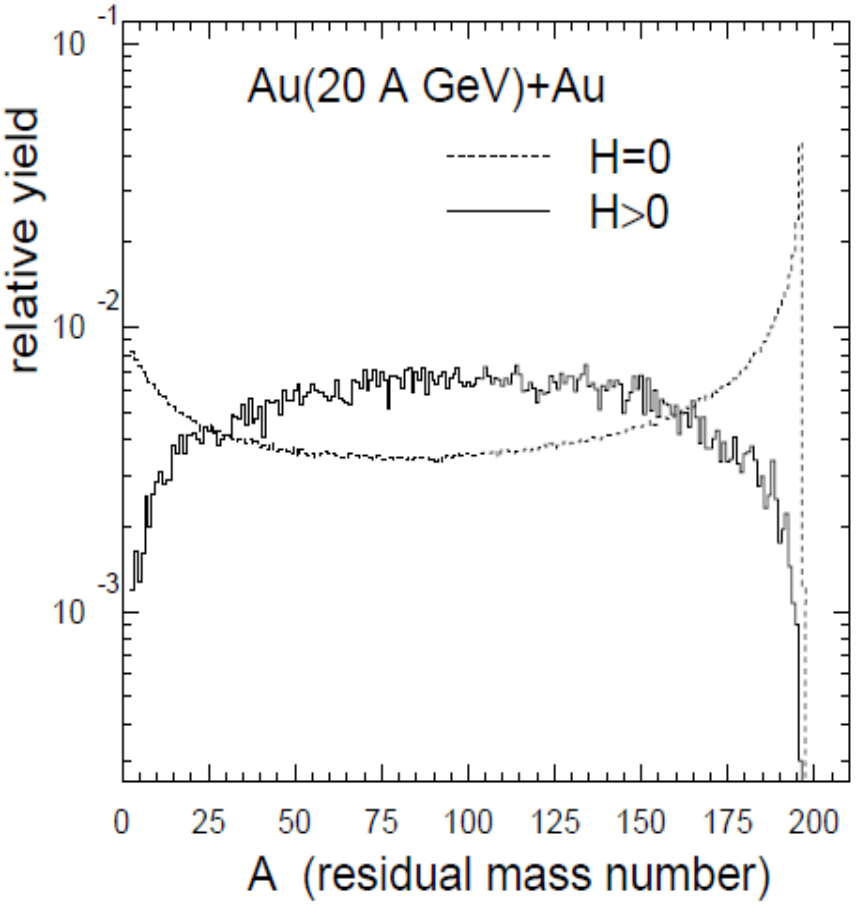

Nuclear system consists of primary clusters in local equilibrium:

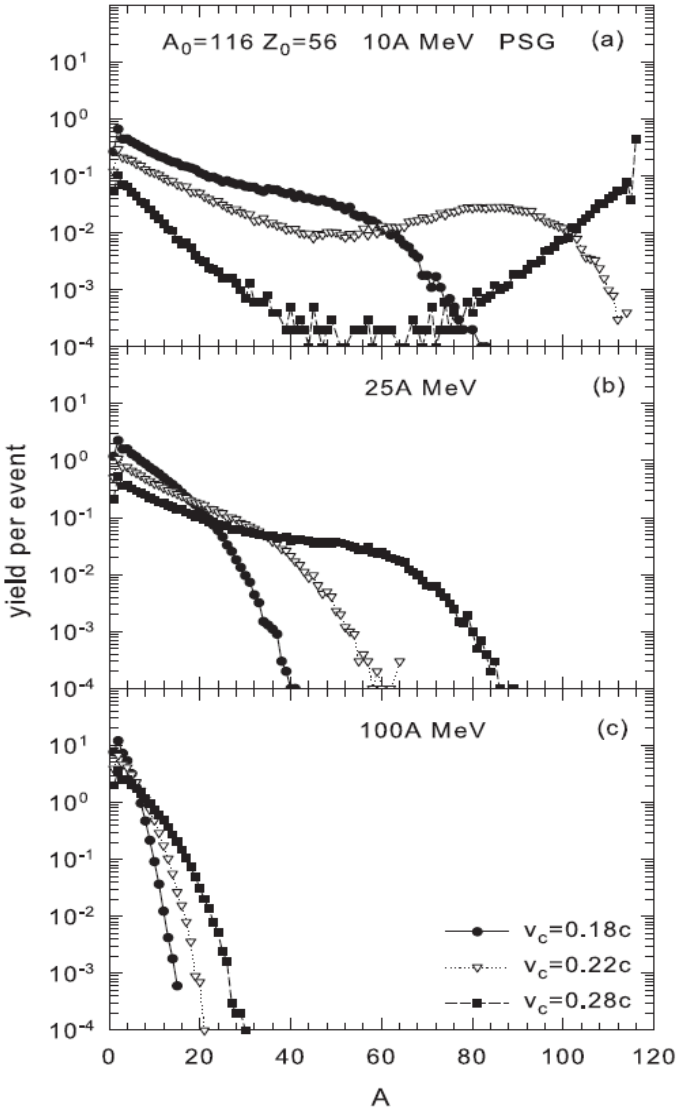

final nuclei after the statistical nucleation (disintegration of the excited clusters via SMM):

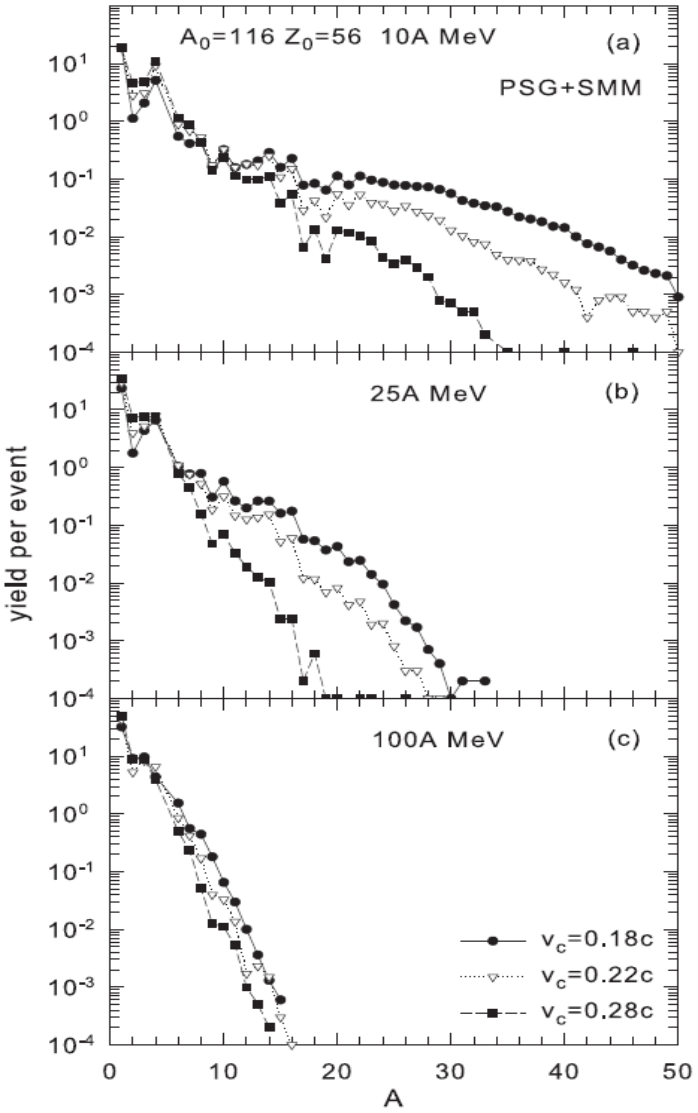

A mechanism for production of novel fragments: Capture of produced baryons by other nucleons and by spectator residues (nuclear matter)

Phenomenological models:

Coalescence (condensation) of baryons into clusters: **CB**

momenta:

$$|Pi - P0| \le Pc$$

coordinates:

$$|Xi - X0| \le Xc$$

Capture in nuclear potential and coalescence are similar mechanisms

Hyperon capture in the spectator potential

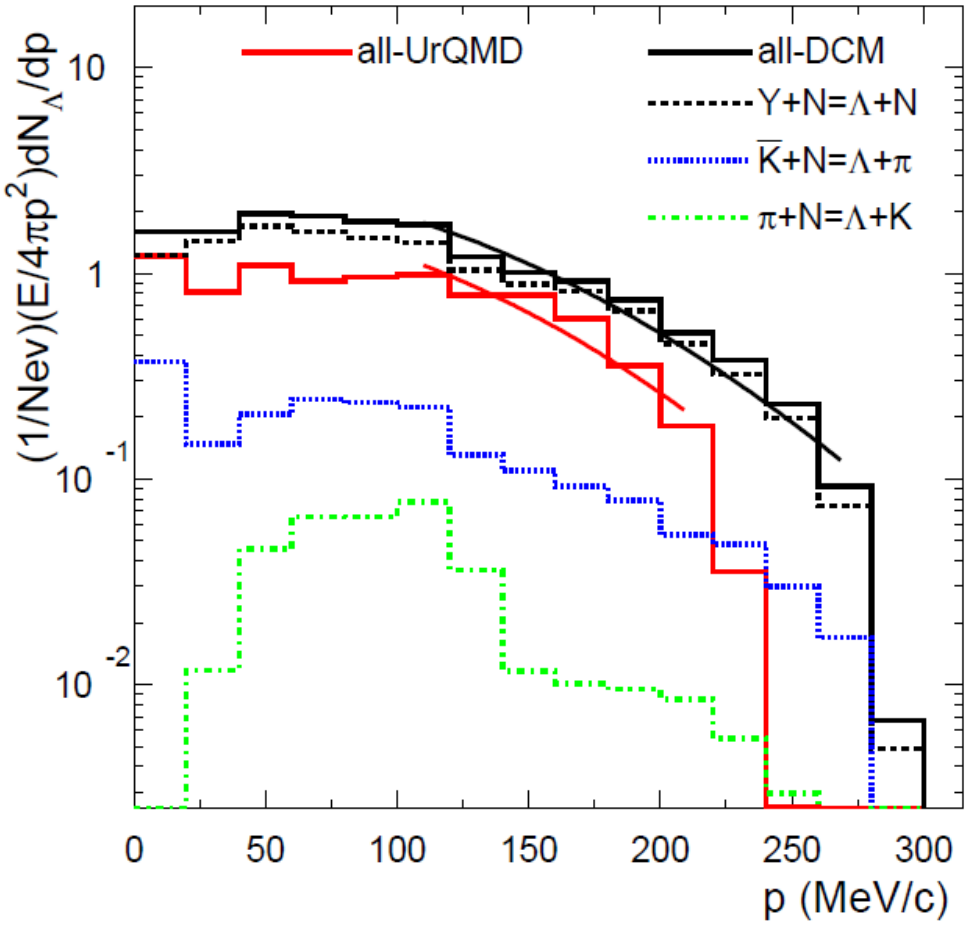

Au(20AGeV)+Au: UrQMD&DCM: PRC**84**, 064904 (2011)

Novel: coalescent fragments can be excited & undergo de-excitation

De-excitation influences mass distributions: Examples for transport (DCM) + coalescence of baryons (CB) + statistical de-excitation (De) calculation. SMM is used.

Velocity coalescent parameter, **Vc=0.22 c** gives their excitation energies around ~10 MeV/nucl.

Final exponential-like decreasing of the mass yields with A.

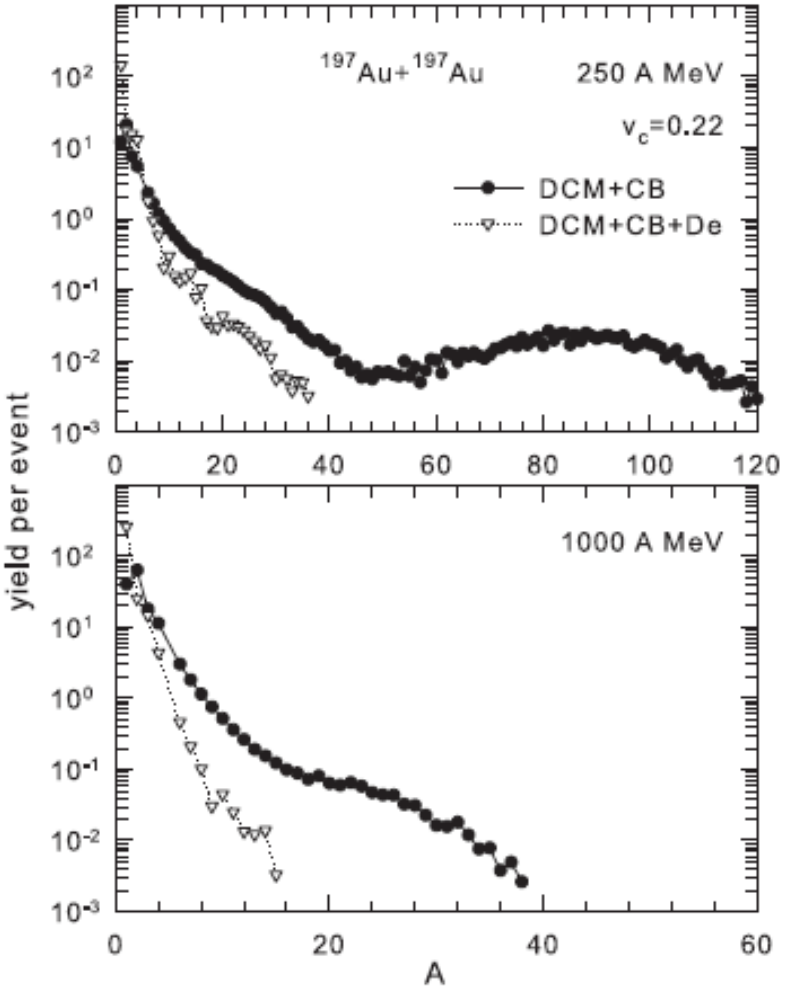

Eur. Phys. J. A 3, 75–83 (1998)

Thermal multifragmentation in p + Au interactions at 2.16, 3.6 and 8.1 GeV incident energies

FASA

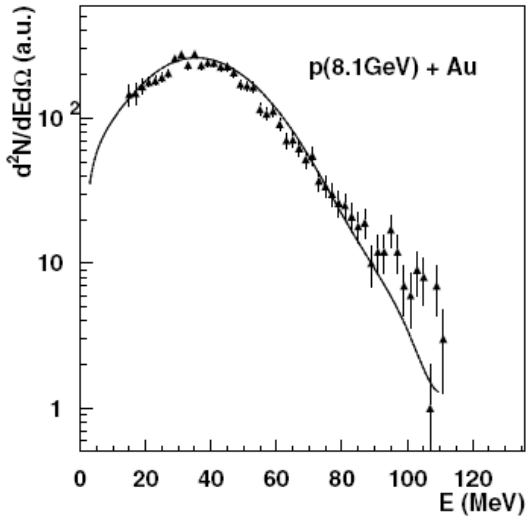

Fig. 8. Energy distribution of carbon isotopes obtained at 8.1 GeV incident energy compared to the one from the INC+Expansion+SMM calculation

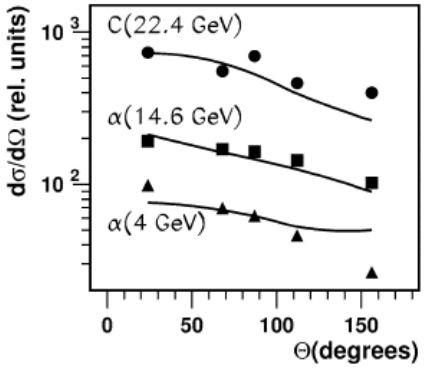

Fig. 9. Angular distributions of carbon (in laboratory system) for ^{4}He + Au and ^{12}C + Au collisions. The lines are calculated with RC + α + SMM.

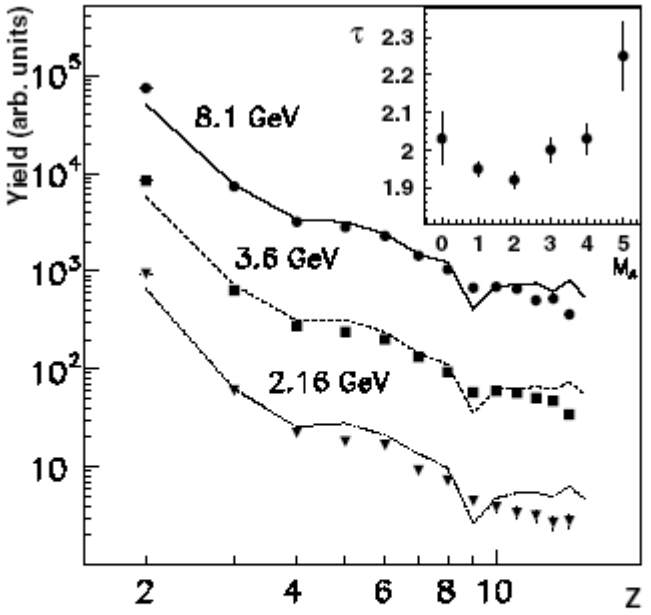

Fig. 10. Fragment charge distributions at the beam energies 8.1 GeV (top), 3.6 GeV (scaled by 1/4) and 2.16 GeV (scaled by 1/16). The lines are calculated by INC+Expansion+SMM (normalized at Z=3). The insert gives the τ-parameter deduced from the IMF-charge spectra for the beam energy of 8.1 GeV as a function of the measured IMF multiplicity

INDRA

Ni+Au 52A MeV

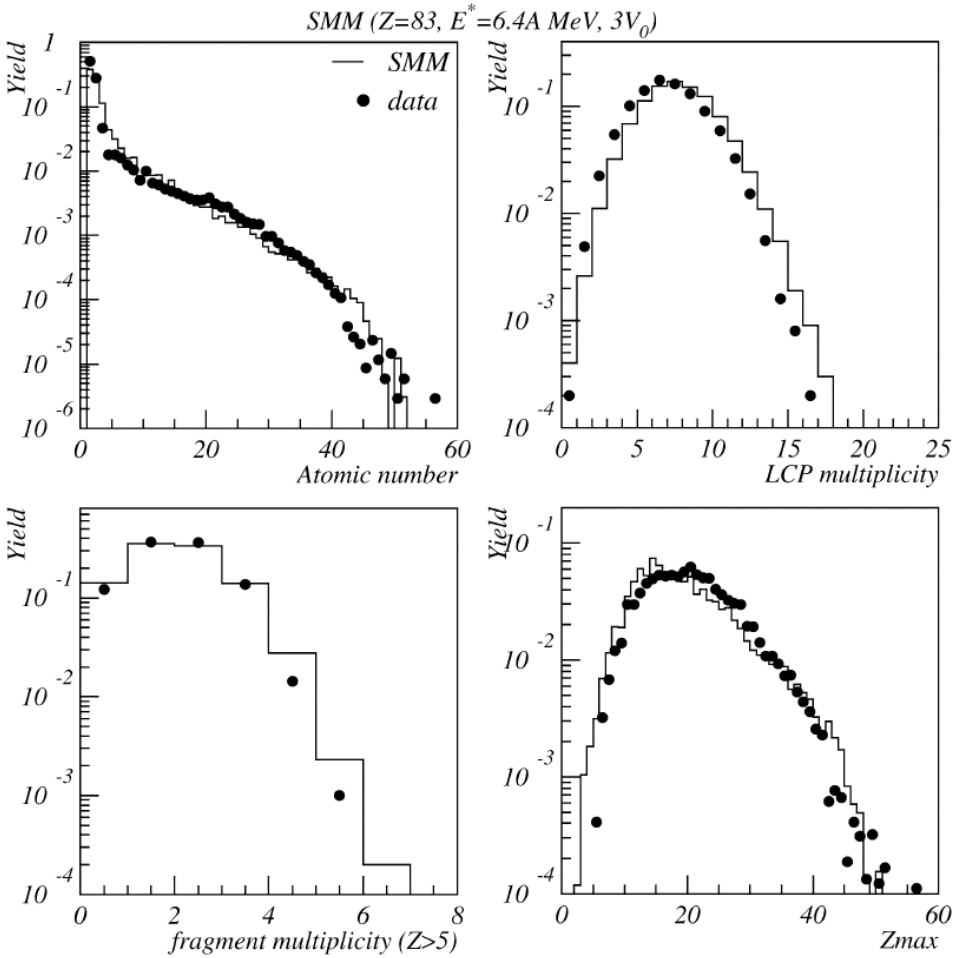

Fig. 10. Atomic number (a) for the 52*A* MeV Ni + Au data (symbols) and SMM (histogram), LCP multiplicity ($Z \leqslant 2$) (b), Fragment multiplicity ($Z \geqslant 6$) (c) and atomic number distributions of the heaviest fragment (d). These comparisons are made in a restricted angular domain in the center of mass (60°–120°). All spectra are normalized to the number of events.

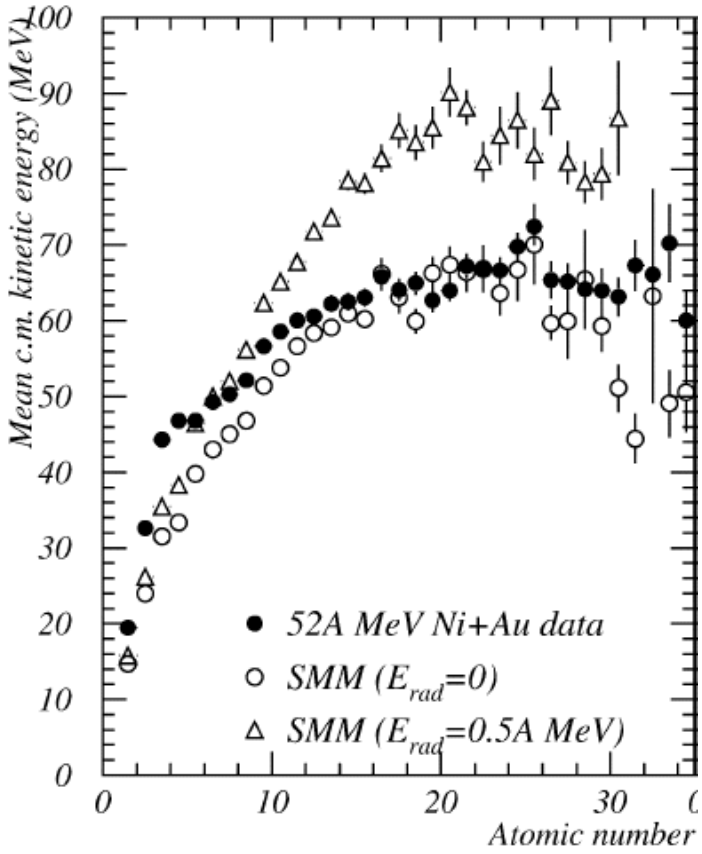

Nuclear Physics A 709 (2002) 367–391